




Cerebral blood flow in 5- to 8-month-olds: Regional tissue maturity is associated with infant affect

M. Catalina Camacho¹  | Lucy S. King² | Amar Ojha² | Cheyenne M. Garcia² |
Lucinda M. Sisk²  | Anna C. Cichocki² | Kathryn L. Humphreys³  | Ian H. Gotlib²

¹Washington University in St. Louis, St. Louis, MO, USA

²Stanford University, Stanford, CA, USA

³Vanderbilt University, Nashville, TN, USA

Correspondence

M. Catalina Camacho, Washington University in St. Louis, St. Louis, MO 63110, USA.

Email: m.catalina.camacho@gmail.com

Funding information

National Institutes of Health, Grant/Award Number: R21 HD090493, R21 MH111978 and F32 MH107129; National Science Foundation; Jacobs Foundation, Grant/Award Number: 2017-1261-05

Abstract

Infancy is marked by rapid neural and emotional development. The relation between brain function and emotion in infancy, however, is not well understood. Methods for measuring brain function predominantly rely on the BOLD signal; however, interpretation of the BOLD signal in infancy is challenging because the neuronal-hemodynamic relation is immature. Regional cerebral blood flow (rCBF) provides a context for the infant BOLD signal and can yield insight into the developmental maturity of brain regions that may support affective behaviors. This study aims to elucidate the relations among rCBF, age, and emotion in infancy. One hundred and seven mothers reported their infants' (infant age $M \pm SD = 6.14 \pm 0.51$ months) temperament. A subsample of infants completed MRI scans, 38 of whom produced usable perfusion MRI during natural sleep to quantify rCBF. Mother-infant dyads completed the repeated Still-Face Paradigm, from which infant affect reactivity and recovery to stress were quantified. We tested associations of infant age at scan, temperament factor scores, and observed affect reactivity and recovery with voxel-wise rCBF. Infant age was positively associated with CBF in nearly all voxels, with peaks located in sensory cortices and the ventral prefrontal cortex, supporting the formulation that rCBF is an indicator of tissue maturity. Temperamental Negative Affect and recovery of positive affect following a stressor were positively associated with rCBF in several cortical and subcortical limbic regions, including the orbitofrontal cortex and inferior frontal gyrus. This finding yields insight into the nature of affective neurodevelopment during infancy. Specifically, infants with relatively increased prefrontal cortex maturity may evidence a disposition toward greater negative affect and negative reactivity in their daily lives yet show better recovery of positive affect following a social stressor.

KEYWORDS

cerebral blood flow, emotion, infant brain development, still-face, temperament

1 | INTRODUCTION

Infancy is marked by rapid neurodevelopment as well as by changes in *affect reactivity*, or emotional responses to stimuli, and *affect regulation*, or the modulation of these responses. Although affect

arises from the dynamic coordination of brain function with the environment, the neural basis of infant affect has yet to be fully characterized. Individual differences in the dispositional tendency toward emotionality (i.e., temperamental emotionality) are apparent from birth (Gartstein & Rothbart, 2003; Putnam, Helbig, Gartstein,

Rothbart, & Leerkes, 2014; Worobey & Blajda, 1989). The systems that regulate emotional functioning emerge later in infancy, however (Shiner et al., 2012). By age 6 months, infants can discriminate among distinct emotions (i.e., they respond differently to different facial expressions or vocal intonations) (Caron, Caron, & MacLean, 1988; Fernald, 1993) and engage in affect regulation including emotion regulation strategies such as gaze aversion (Mangelsdorf, Shapiro, & Marzolf, 1995). Measures of infant temperamental emotionality become more stable with increasing infant age (Shiner et al., 2012), suggesting the development of a stable profile of affect reactivity and regulation that is bi-directionally associated with ongoing brain maturation. Importantly, individual differences in affect reactivity and regulation during infancy predict later social and academic competence (Belsky, Friedman, & Hsieh, 2001) and symptoms of psychopathology (Crockenberg, Leerkes, & Barrig Jo, 2008; Miller, Degnan, Hane, Fox, & Chronis-Tuscano, 2018). Therefore, elucidating the associations between infant affect reactivity and regulation and infant brain function may reveal early biobehavioral signatures of risk for, or resilience to, future difficulties.

During the first year of life, the cortical surface expands by an average of 76% (Li et al., 2013), cerebral gray matter doubles in volume (Knickmeyer et al., 2008), and components of adult-like higher level networks present at birth begin to integrate across hemispheres and lobes (Doria et al., 2010; Fransson et al., 2007; Gao, Alcauter, Elton, et al., 2015; Gao et al., 2011). The parietal and prefrontal cortices develop rapidly during the first year of life, with acceleration of prefrontal cortex (PFC) development that continues through the toddler years (Gao, Alcauter, Elton, et al., 2015; Wen et al., 2019) in concert with the development of basic attention systems and improved integration of multimodal information (Morales, Fu, & Pérez-Edgar, 2016; Posner, Rothbart, Sheese, & Voelker, 2014). Studies using methods that provide recordings of cortical surface activation, such as functional near-infrared spectroscopy (fNIRS) and electroencephalogram (EEG), indicate a shifting role of the cortex in discriminating and responding to the emotional facial expressions of others between the ages of 4 and 7 months. Specifically, whereas in 4-month-olds there is no difference in cortical activation in response to happy, angry, or neutral facial expressions (Striano, Kopp, Grossmann, & Reid, 2006), by 7 months of age there is evidence that dorsolateral PFC activation supports attention to emotional faces (Grossmann, Missana, & Krol, 2018) and that temporal cortex spatial activation distinguishes happy from angry faces and voices (Grossmann, Striano, & Friederici, 2005; Nakato, Otsuka, Kanazawa, Yamaguchi, & Kakigi, 2011).

Although findings of studies using fNIRS and EEG suggest that there is an important neurodevelopmental shift in emotion processing between ages 4 and 7 months, these methods are limited to recordings of the superficial cortex (fNIRS) or across the brain that is then projected onto the cortical surface (EEG). Indeed, fNIRS and EEG cannot reveal the functional interactions among subcortical and cortical limbic, sensory integration, and prefrontal regions that are likely to be critical for affect reactivity and regulation in infancy (Damasio et al., 2000; Lindquist, Wager, Kober, Bliss-Moreau, & Barrett, 2012; Pessoa, 2017). Given that attentional deployment

Research Highlights

- An exploratory factor analysis of infant temperament yielded three factors: negative affect, surgency, and soothability.
- Infant age is positively associated with regional cerebral blood flow throughout the brain with peak regions in primary sensory cortices.
- Infant recovery of positive affect post-stressor is associated with increased blood flow in regions supporting automatic regulation: the inferior frontal gyri and orbitofrontal cortex.
- Temperamental Negative Affect is associated with increased blood flow in the medial orbitofrontal cortex even after correcting for global blood flow.

(e.g., gaze orientation) is a dominant form of affect regulation during infancy (Thomas, Letourneau, Campbell, Tomfohr-Madsen, & Giesbrecht, 2017), researchers have hypothesized that the salience network attentional systems largely support affect regulation during this period (Rothbart & Posner, 2015; Rothbart, Sheese, Rueda, & Posner, 2011). Findings from studies using blood oxygenation level dependent (BOLD) functional magnetic resonance imaging (fMRI) to examine infant cortical and subcortical brain function suggest that although adult-like primary sensory networks are present as young as one month of age, the default mode and salience networks do not evidence adult-like integration across hemispheres and major lobes (i.e., prefrontal to parietal) until age 6 months (Gao, Alcauter, Elton, et al., 2015). Seed-based analyses probing limbic subcortical to prefrontal circuitry indicate that functional connectivity between the amygdala and the PFC increases dramatically during the first year of life (Salzwedel et al., 2018). While there is evidence that the PFC supports cognitive function in infants (Grossmann & Johnson, 2010; Linke et al., 2018; Striano et al., 2006), there is little research examining whether variation in the maturity of sensory, limbic, and prefrontal circuitry is associated with differences in affect reactivity and regulation in infancy. In the only study to our knowledge to examine infant affect in this context, Graham, Pfeifer, Fisher, Carpenter, and Fair (2015) found that greater functional connectivity between default mode network regions at age 6–12 months was associated with parent-reported negative emotionality assessed at the same timepoint.

In both the broader infant MRI literature and in investigations focused on infant neural circuitry involved in emotion, research has been hampered by two limitations of prevailing infant MRI methods. First, there is a “flip” in relative MRI-derived white and gray matter tissue contrast that occurs in humans at around 5–9 months (Paus et al., 2001; Wang et al., 2015) that is characterized by both a greater distinction in T1 and T2 white/gray matter contrast and a dramatic increase in white matter T1 and decrease in white matter T2. This sharp change in T1/T2 values likely results from the sharp increase

in synaptic (Huttenlocher, 1990; Huttenlocher, de Courten, Garey, & Van der Loos, 1982) and capillary density in gray matter (Harb, Whiteus, Freitas, & Grutzendler, 2013; Norman & O'kusky, 1986) as well as from increased myelination in white matter (Dean et al., 2016; Geng et al., 2012) during this developmental period. Second, neuronal-hemodynamic coupling develops nonlinearly during infancy (Kozberg, Chen, DeLeo, Bouchard, & Hillman, 2013; Kozberg & Hillman, 2016). This second limitation is particularly important when considering fMRI measures of brain function that rely on the BOLD signal. BOLD fMRI quantifies brain activation using the paramagnetic signal from deoxygenated hemoglobin (Hb) in which a decrease in Hb corresponds to a positive BOLD response. The interpretation that the BOLD response indicates activation is based on studies that identify coupling between firing of a neuronal population and an initial increase in Hb followed by an increase in overall blood flow to the area, resulting in decreased concentration of deoxygenated Hb relative to oxygenated Hb (Arthurs & Boniface, 2002; Hillman, 2014; Logothetis, Pauls, Augath, Trinath, & Oeltermann, 2001). It is unclear, however, at what age this stereotyped neuronal-hemodynamic response emerges in humans. Indeed, human infant task-based fMRI and fNIRS studies have identified a mixture of both positive and negative hemodynamic responses to environmental stimuli (Arichi et al., 2012, 2010; Born et al., 2000; Deen et al., 2017; Issard & Gervain, 2018; Meek et al., 1998; Minagawa-Kawai et al., 2011; Yamada et al., 1997), suggesting that, unlike adults, brain activity in infants can be reflected as either increased or decreased BOLD. Recent work with rats indicates that neuronal-hemodynamic coupling is not well established until rats are past postnatal day 23 (Kozberg et al., 2013; Kozberg & Hillman, 2016), analogous to 5–12 months in humans (Sengupta, 2013). Thus, continued development of neuronal-hemodynamic coupling during infancy in combination with shifts in the tissue content – gray matter increasing in density and white matter increasing in fat content – that influence T2* signal contrast could explain the equivocal findings in the human infant literature.

To extend previous research and increase our understanding of the neural basis of infant affect, the current study aimed to identify regions of the healthy infant brain that are functionally related to affect reactivity and regulation at ages 5–8 months. To characterize infant affect, we assessed both temperamental emotionality (i.e., global) and situational (i.e., in response to laboratory stress) affect reactivity and regulation using parent-report and observational measures, respectively. Whereas parent-report measures may be biased by variations in both maternal characteristics and the caregiving environment, laboratory-based observational measures may provide information about infants' *capacity* to engage in certain behaviors rather than about their *tendency* to engage in these behaviors in daily life. Therefore, we think that examining both temperamental emotionality and situational affect reactivity and regulation in association with neural data provides complementary insight into infant affective neurodevelopment. To characterize infant brain function, we assessed regional cerebral blood flow (rCBF) using pseudocontinuous arterial spin labeling (ASL). We used rCBF because it is independent of the BOLD signal, can be measured non-invasively, and is

less susceptible than is BOLD fMRI to age-related changes in underlying T2 signal. ASL labels blood as it passes through the neck and images the signal from the labels after perfusion. Given that capillary perfusion in the brain is still developing in infancy (Harb et al., 2013; Norman & O'kusky, 1986), greater rCBF during this period may indicate greater tissue maturity. Therefore, indexing regional tissue maturity in relation to affective behavior may provide insight into the development of circuits that support affective function in early life. In this study, we tested the hypothesis that infant age is positively associated with rCBF across the brain. We then explored the associations between rCBF and temperamental and situational measures of infant affect reactivity and regulation. Because the brain does not develop at a uniform rate for all individuals, individual differences in infant rCBF above and beyond differences explained by chronological age may indicate relative tissue maturity.

2 | METHODS

2.1 | Participants

One hundred and nine mother–infant dyads were recruited from Bay Area communities to take part in a study of caregiving and infant neural and behavioral development (see Humphreys, King, Choi, & Gotlib, 2018; King, Humphreys, & Gotlib, 2019). The current analyses include the 107 mothers (19.51–45.64 years old) and their infants ($M \pm SD$ age = 6.14 ± 0.51 months) who completed a parent-report assessment of their infants' temperament. We present detailed characteristics of the sample in Table 1. All 107 infants were included in a factor analysis to derive dimensions of infant temperamental emotionality (see Section 5); of these infants, 97 completed the repeated Still-Face Paradigm (see Section 6) and 38 ($M \pm SD$ age = 6.62 ± 0.61 months) provided usable MRI data for neuroimaging analyses. Compared to infants who did not provide usable MRI data, infants who provided usable data did not differ in age, race, ethnicity, sex, or breastfeeding status or in maternal race, ethnicity, education level, or annual household income ($ps > 0.05$).

2.2 | Study procedure

This study was approved by the Institutional Review Board at Stanford University and written consent was obtained from mothers. To participate, interested mothers were first interviewed over the phone to assess study eligibility. Inclusion criteria were having an infant between the ages of 5 and 8 months, being fluent in English, having no immediate plans to move away from the geographic area. Exclusion criteria included maternal bipolar disorder, maternal psychosis, maternal severe learning disabilities, severe complications during birth, infant head trauma, infant premature birth (prior to 36 weeks gestation), and infant MRI contraindication (such as an implant). Eligible dyads first completed a laboratory session in which mothers responded to questionnaires and

TABLE 1 Sample demographics

	Temperament analysis (N = 107)	Included in CBF analysis (N = 38)	Unusable for CBF analysis (N = 42)	Statistic <i>p</i> -value
Demographics				
Infant age, mean \pm SD months	6.14 \pm 0.51	6.62 \pm 0.61	6.75 \pm 0.52	$t(78) = 1.07$ $p = .255$
Infant race, number (percent)				$\chi^2(4) = 4.23$ $p = .376$
White/Caucasian American	61 (57.0)	23 (60.5)	24 (57.1)	
Asian American	21 (19.6)	8 (21.1)	7 (16.7)	
Black/African American	4 (3.7)	3 (7.9)	1 (2.4)	
Native Hawaiian/Pacific Islander	1 (0.9)	0 (0.0)	0 (0.0)	
American Indian or Alaska Native	1 (0.9)	0 (0.0)	0 (0.0)	
Other/biracial	16 (15.0)	4 (10.5)	8 (19.0)	
Decline to state	3 (2.8)	0 (0.0)	2 (4.8)	
Infant ethnicity, number (percent)				$\chi^2(3) = 0.29$ $p = .866$
Hispanic or Latino	21 (19.6)	9 (23.7)	9 (21.4)	
Not Hispanic or Latino	82 (76.6)	28 (73.7)	31 (73.8)	
Decline to State	4 (3.7)	1 (2.6)	2 (4.8)	
Infant sex, N male (percent)	51 (47.7)	21 (55.3)	19 (45.2)	$\chi^2(1) = 0.80$ $p = .370$
Breastfed, number (percent)				$\chi^2(2) = 3.83$ $p = .147$
Yes	96 (89.7)	33 (86.8)	38 (90.5)	
No	4 (3.7)	3 (7.9)	0 (0.0)	
Decline to state	7 (6.5)	2 (5.3)	4 (9.5)	
Mother age, mean \pm SD years	33.49 \pm 4.72	33.36 \pm 4.85	33.57 \pm 5.44	$t(78) = 0.18$ $p = .856$
Maternal race, number (percent)				$\chi^2(3) = 0.08$ $p = .994$
White/Caucasian American	67 (62.6)	24 (63.2)	26 (61.9)	
Asian American	25 (23.4)	9 (23.7)	11 (26.2)	
Black/African American	2 (1.9)	1 (2.6)	1 (2.4)	
Native Hawaiian/Pacific Islander	1 (0.9)	0 (0.0)	0 (0.0)	
American Indian or Alaska Native	1 (0.9)	0 (0.0)	0 (0.0)	
Other/biracial	11 (10.3)	4 (10.5)	4 (9.5)	
Decline to state	0 (0.0)	0 (0.0)	0 (0.0)	
Maternal ethnicity, number (percent)				$\chi^2(1) = 0.42$ $p = .519$
Hispanic or Latino	17 (15.9)	6 (15.8)	9 (21.4)	
Not Hispanic or Latino	90 (84.1)	32 (84.2)	33 (78.6)	
Decline to state	0 (0.0)	0 (0.0)	0 (0.0)	
Maternal education, number (percent)		M rank = 44.9	M rank = 36.5	$H(1) = 3.15$ $p = .076$
Some high school	1 (0.9)	0 (0.0)	1 (2.4)	
High school diploma/GED	0 (0.0)	0 (0.0)	0 (0.0)	
Some college	7 (6.5)	0 (0.0)	5 (11.9)	
Associate's degree	5 (4.7)	1 (2.6)	3 (7.1)	

(Continues)

TABLE 1 (Continued)

	Temperament analysis (N = 107)	Included in CBF analysis (N = 38)	Unusable for CBF analysis (N = 42)	Statistic <i>p</i> -value
Trade/technical school	2 (1.9)	2 (5.3)	0 (0.0)	
Bachelor's degree	37 (34.6)	13 (34.2)	15 (35.7)	
Graduate degree	55 (51.4)	22 (57.9)	18 (42.9)	
Annual household income, number (percent)		M rank = 37.9	M rank = 42.9	$H(1) = 1.07$ $p = .302$
Less than \$5,000	0 (0.0)	0 (0.0)	0 (0.0)	
\$5,001–15,000	1 (0.9)	0 (0.0)	1 (2.4)	
\$15,001–30,000	4 (3.7)	2 (5.3)	2 (4.8)	
\$30,001–60,000	12 (11.2)	6 (15.8)	4 (9.5)	
\$60,001–90,000	7 (6.5)	2 (5.3)	2 (4.8)	
\$90,001–150,000	26 (24.3)	12 (31.6)	10 (23.8)	
More than \$150,000	56 (52.3)	16 (42.1)	22 (52.4)	
Decline to state	1 (0.9)	0 (0.0)	1 (2.4)	
IBQ-R-SF temperament				
Activity level	4.26 ± 0.95	4.32 ± 1.06	4.25 ± 0.91	$t(78) = -0.31$ $p = .760$
Approach	5.59 ± 0.87	5.56 ± 0.80	5.63 ± 0.87	$t(78) = 0.34$ $p = .734$
Cuddliness	5.84 ± 0.79	5.98 ± 0.67	5.72 ± 0.80	$t(78) = -1.57$ $p = .121$
Distress to limitations	3.81 ± 0.98	3.67 ± 0.85	4.05 ± 1.14	$t(78) = 1.69$ $p = .096$
Duration of orienting	3.86 ± 1.05	3.81 ± 1.08	3.93 ± 1.11	$t(78) = 0.49$ $p = .625$
Falling reactivity	5.18 ± 0.91	5.36 ± 0.81	4.93 ± 1.00	$t(78) = -2.08$ $p = .038$
Fear	2.51 ± 1.15	2.34 ± 0.92	2.56 ± 1.25	$t(78) = 0.89$ $p = .376$
High intensity pleasure	6.10 ± 0.78	6.10 ± 0.79	6.02 ± 0.74	$t(78) = -0.46$ $p = .648$
Low intensity pleasure	5.41 ± 0.84	5.36 ± 0.74	5.49 ± 0.98	$t(78) = 0.71$ $p = .482$
Perceptual sensitivity	4.17 ± 1.54	3.96 ± 1.75	4.26 ± 1.19	$t(78) = 0.87$ $p = .389$
Sadness	3.40 ± 1.03	3.42 ± 0.93	3.64 ± 0.98	$t(78) = 1.00$ $p = .322$
Smiling and laughter	4.61 ± 1.07	4.49 ± 1.14	4.51 ± 0.94	$t(78) = 0.09$ $p = .926$
Soothability	5.73 ± 0.75	5.71 ± 0.71	5.64 ± 0.76	$t(78) = -0.40$ $p = .690$
Vocal reactivity	4.83 ± 1.00	4.64 ± 1.16	4.88 ± 0.91	$t(78) = 1.03$ $p = .306$
SFP-R affect				
Negative affect reactivity, Mean ± SD seconds	52.98 ± 54.32	61.92 ± 54.37	46.59 ± 51.99	$t(71) = -1.23$ $p = .223$
Positive Affect Recovery, Mean ± SD seconds	29.00 ± 26.88	24.93 ± 24.90	30.50 ± 25.50	$t(71) = 0.94$ $p = .348$

Note: Descriptive demographics and statistical comparisons of infants who did and did not produce usable ASL data are included in the shaded area of the table (of the 80 total whose mothers elected for them to participate in the MRI scan session).

Abbreviations: CBF, cerebral blood flow; IBQ-R-SF, Infant Behavior Questionnaire-Revised Short Form; SFP-R, Still-Face Paradigm.

dyads completed the repeated Still-Face Paradigm (described below). Following the laboratory session, dyads were invited to participate in an infant MRI scan. Of the 107 dyads, 80 agreed to participate in an MRI brain scan session, of whom 38 provided complete and usable data for the analysis of rCBF. The MRI scans were completed an average of 2.94 ($SD = 1.97$) weeks after the laboratory session.

2.3 | Infant temperamental affect

Mothers completed the short form of the Infant Behavioral Questionnaire-Revised (IBQ-R-SF) (Putnam et al., 2014), a reliable and valid measure of infant temperament. The IBQ-R-SF is composed of 13 subscales that assess infants' tendencies toward reactivity, emotionality, and regulation. The original IBQ-R found that these 13 subscales clustered into three factors including surgency (made up of the Approach, Vocal Reactivity, High Intensity Pleasure, Smiling and Laughter, Activity, and Perceptual Sensitivity Subscales), Negative Affect (the Sadness, Distress to Limitations, Fear, and negatively loaded Falling Reactivity and High Intensity Pleasure subscales), and self-regulation (Low Intensity Pleasure, Cuddliness, Soothability, Duration of Orienting, Smiling and Laughter, and negatively loaded Distress to Limitations subscales) (Gartstein & Rothbart, 2003; Putnam et al., 2014).

To characterize dimensions of temperamental emotionality specific to the current sample, we conducted an exploratory factor analysis (EFA) using the psych library (Revelle, 2018) in R v3.3 and varimax rotation. We chose to conduct a sample-specific EFA given evidence that the factor structure of the IBQ-R differs in demographically diverse samples (the original IBQ-R was largely developed in relatively homogenous samples; Bosquet Enlow, White, Hails, Cabrera, & Wright, 2016). For comparison and potential meta-analytic purposes, however, we include in Appendix I an analysis using the original factor scores (Table A1). To determine the appropriate number of factors to model, we conducted a parallel analysis of simulated data (Ruscio & Roche, 2012) and inspected the resulting scree plot. We used the number of factors at the elbow of the curve in a subsequent EFA model. We determined model fit according to recommended guidelines in the field (Schreiber, Nora, Stage, Barlow, & King, 2006) with a Tucker-Lewis index (TLI) greater than or equal to 0.95, root mean square error of approximation (RMSEA) less than or equal to 0.08, and a standardized root mean square residual (SRMSR) less than or equal to 0.08 indicating an excellent fit. For each infant, we computed factor scores for each of the identified factors, that we used as the measures of temperamental affect in subsequent analyses. Based on published guidelines from EFA simulations (de Winter et al., 2009), we were well-powered to detect loadings that are at least 0.5 with our sample of 107 infants and three factors (note that the characteristics of this analysis fell between the 0.4 and 0.6 loading sizes provided in the published guidelines).

2.4 | Infant situational affect

During the laboratory session, infants and their mothers completed the repeated Still-Face Paradigm (SFP-R) (Haley & Stansbury, 2003; Tronick, Als, Adamson, Wise, & Brazelton, 1978). The SFP-R consists of five two-minute face-to-face interaction episodes between mother and child: (a) a baseline normal play episode; (b) the still-face episode in which mothers become unresponsive and maintain a neutral expression without touching their infant; (c) a reunion episode in which mothers resume normal interaction; (d) a second still-face episode; and (e) a final reunion episode. The repeated and non-repeated versions of the SFP-R consistently produce a pattern of increased negative affect during the still-face episodes relative to the play and reunion episodes, which is interpreted as Negative Affect Reactivity to the "stressor" of maternal disengagement, as well as decreased positive affect during the reunion episodes relative to the play episode, which is interpreted as an individual difference variable reflecting the degree of recovery of positive affect following the stressor (hereafter termed "Positive Affect Recovery;" Mesman, van IJzendoorn, & Bakermans-Kranenburg, 2009).

In the current study, separate cameras recorded mother and infant for the SFP-R. Recordings were then time-locked in Datavyu (Datavyu Team, 2014) and coded for infant affect on a second-by-second basis from infant facial expressions, vocalizations, and body movement (Bosquet Enlow et al., 2012) by one of two trained raters (ICC = 0.91; see Appendix II for further details) masked to mother-reported temperament and the neuroimaging analysis. We followed previously published methods (Bosquet Enlow et al., 2012) to quantify infant negative and positive affect during each episode of the SFP-R. Specifically, to quantify negative affect we first computed the proportion of time the infant was fussing, crying, and hard crying (i.e., number of seconds in each state/duration of the episode) and then calculated a weighted sum of negative affect as follows:

$$\text{Negative affect} = P(\text{fussing}) + 2 * P(\text{crying}) + 3 * P(\text{hard crying})$$

Similarly, to quantify positive affect, we computed the proportion of time that the infant exhibited positive and very positive affect and calculated a sum where the proportion of very positive affect was weighted by a factor of 2.

$$\text{Positive affect} = P(\text{positive affect}) + 2 * P(\text{very positive affect})$$

In order to capture affect dynamics across the SFP-R, we calculated indices of Negative Affect Reactivity and Positive Affect Recovery. Negative Affect Reactivity was operationalized as infant negative affect during each still face (SF) episode subtracted from the preceding non-SF (i.e., play [P]; reunion 1 [R1]; reunion 2 [R2]) episode and averaged:

$$\text{Reactivity} = \frac{(\text{SF1 neg. affect} - P \text{ neg. affect} + \text{SF2 neg. affect} - R1 \text{ neg. affect})}{2}$$

Higher scores of Negative Affect Reactivity indicate greater increases in negative affect from non-still-face to still-face episodes. Positive Affect Recovery was operationalized as infant positive affect during each reunion (i.e., "recovery") episode subtracted from positive affect during the preceding still-face episode and averaged:

$$\text{Recovery} = \frac{(\text{R1 pos. affect} - \text{SF1 pos. affect} + \text{R2 pos. affect} - \text{SF1 pos. affect})}{2}$$

Higher scores of Positive Affect Recovery indicate relatively larger levels of positive affect in the reunion relative to SF episodes. We focused on recovery of positive affect primarily for methodological reasons. Positive Affect Recovery and Negative Affect Reactivity captured distinct variation in infant affect regulation and reactivity ($r = .18$). In contrast, Negative Affect Recovery was strongly correlated with Negative Affective Reactivity (full sample: $r = .60, p < .001$; neuroimaging sample: $r = .54, p = .001$).

Of the 107 mother–infant dyads who participated in this study, ten did not complete the SFP-R, four were not coded for infant affect, and ten completed only one each of the still-face and reunion episodes. For the dyads that partially completed the SFP-R, affect ratings from the play, first reunion, and first still-face episodes were used to quantify Negative Affect Reactivity and Positive Affect Recovery. All 38 infants included in the CBF analysis completed the SFP-R (32 completed the full paradigm, six completed only one still-face and one reunion episodes). An examination of the association between each of the infant affect measures and caregiving behaviors coded from the SFP-R interactions is included in Appendix III (Table A2; Figures A1 and A2).

2.5 | MR imaging acquisition

Mothers who chose to participate in the MRI session were given an MRI prep kit to prepare their infants for the MRI session during the week preceding the scheduled scan date. This kit included two sets of earplugs and a small portable speaker pre-loaded with MRI sounds. Mothers were encouraged to put the ear plugs in their infant's ears and play the MRI sounds during play and naptime to acclimate the infant. If the mothers did not swaddle their infants, they were encouraged to start swaddling their infant for sleep. On the day of the scan, dyads arrived at the scanner approximately 30 min before the infant's normal bed time. Infants were undressed and changed into a disposable diaper, swaddled in a muslin cloth, and placed in a MedVac Immobilizer designed for infants. After the infant was buckled in, but before the air was removed from the immobilizer, earplugs were placed in the infant's ears and held in place with skin-safe medical tape. Infants who tolerated headphones or slept with white noise were given active noise cancelling headphones playing white noise as additional hearing protection. Infants who did not tolerate headphones were instead given Natus Medical neonatal noise attenuators (miniMuffs) with

additional skin-safe tape to keep them in place. Next, the air was removed from the immobilizer and the infant was soothed and fed per his/her usual bedtime routine. Once the infant had been sleeping for 10 min, the infant was transferred to the MRI scanner bed. If the infant remained asleep during transition and for the next 5 min, MRI acquisition was initiated. Acquisition was stopped if the infant woke up and was restarted after the infant had once again been sleeping soundly for 10 min. This process continued until all sequences were collected, or the infant's parent wanted to stop scanning for the night, or the infant refused to soothe or sleep in the scanner room. A staff member remained with the infant at all times, including in the scanner room, watching for distress and to soothe the infant if he/she started to stir or wake up.

MR images were collected using a 3 Tesla GE MR750 Discovery scanner equipped with a 32-channel NovaMedical head coil. In order to estimate rCBF, pseudocontinuous ASL data were collected using GE's 3DASL pulse sequence diagram (3.0 mm × 2.0 mm × 2.0 mm voxel, 44 axial slices, 10 spiral arms, 512 points, TR = 4,674 ms, TE = 11 ms, flip angle = 111 degrees, FOV = 240 mm), which is comprised of a perfusion acquisition (NEX = 3, Post-Label Delay = 1525 ms, Labeling Time = 1,450 ms, 4 acquisitions) followed by a complementary proton density-weighted volume (PD). The sequence was collected at the end of a longer MRI acquisition session. To ensure standardized placement of the labeling plane, the inferior edge of the imaging volume's sagittal prescription window was aligned with the inferior aspect of each infant's cerebellum. This ensured that the labeling plane consistently captured the right and left internal carotid arteries and the basilar artery at a standardized distance from the brain. As part of the sequence, the label-control perfusion images were time-averaged across all acquisitions to produce a single perfusion-weighted volume (PW). High-resolution T2-weighted (T2w) images were collected within the same session using a 3D fast spin echo sequence (1 mm × 1 mm × 0.8 mm voxel, 204 sagittal slices, 256 × 256 acquisition matrix, flip angle = 90 degrees, FOV = 256 mm, TR = 2,502 ms, TE = 91.4 ms). Data were visually inspected for artifacts prior to data processing. Of the 80 infants who attempted the MRI scan, 30 failed to sleep on the scanner bed and, therefore, did not enter the scanner at all. Of the 50 infants who successfully entered the scanner and slept through at least one sequence, 43 remained asleep until the ASL sequence at the end of the protocol. Of these 43 infants, two woke up during ASL acquisition without returning to sleep, one did not provide a complete acquisition (the superior cortex was cut off), and two were excluded due excessive motion. Therefore, the final analysis included 38 infants.

2.6 | MR data processing and CBF quantification

T2w anatomical images (hereafter referred to as T2w) were processed using iBEAT v1 (Dai, Shi, Wang, Wu, & Shen, 2013). T2w images were corrected for nonuniformity in intensities,

skull-stripped, and resampled to 2 mm isotropic voxels. CBF quantification and analysis was carried out using the NiPype framework (Gorgolewski et al., 2011) in Python v3.4. The full code can be found at https://github.com/catcamacho/infant_pcasl. Each raw PW and PD volume were registered to the T2w, resliced to 2 mm isotropic voxels, and skull-stripped. The resulting PW and PD images were used to quantify CBF in $\text{ml } 100 \text{ g}^{-1} \text{ min}^{-1}$ (Alsop et al., 2015). The kinetic modeling equation is reproduced below with the specifics for this study:

$$\text{CBF} = \frac{6000 * \lambda * \text{PW} * e^{\frac{\text{PLD}}{\text{T}_{1\text{blood}}}}}{\text{T}_{\text{saturation}} * \alpha * \text{NEX} * \text{T}_{1\text{blood}} * \text{PD} * \left(1 - e^{-\frac{\text{LT}}{\text{T}_{1\text{blood}}}}\right)},$$

where λ is the blood–brain partition coefficient (whole brain average 0.9 ml/g), α is the labeling efficiency (0.6; obtained from GE and defined as the inversion efficiency multiplied by the background suppression efficiency at the scanner), $\text{T}_{\text{saturation}}$ is the estimated time it takes for tissue to saturate (2 s), and $\text{T}_{1\text{blood}}$ is the estimated T1 of blood at a 3T scanner (1.6 s). To account for the acquisition parameters specific to the scanner, the PD volume was scaled by the following factors per GE's recommendations before being included in the above equation:

$$\text{PD} = \frac{1}{1 - e^{-\frac{\text{TR}}{\text{T}_{1\text{tissue}}}}} * 32 * \text{PD}_{\text{raw}},$$

where $\text{T}_{1\text{tissue}}$ is a voxel-wise estimated T1 signal. To ensure accuracy of the $\text{T}_{1\text{tissue}}$ volume to this specific sample of infants, a template was created from a subset of infants who additionally had quantitative T1 MRI data (see Appendix IV for detailed procedures including sample demographics in Table A3 and images of the template in Figure A3). Next, the T2w image was registered to a sample-specific template T2w brain and the resulting transformation was applied to the CBF volume. Due to the poor signal quality in white matter collected using ASL (Alsop et al., 2015), all subsequent analyses were limited to gray matter only. A generous gray matter mask was created from the T2w template brain by thresholding to exclude intensity values that are 100% likely to be white matter, dilating the resulting mask by 1 and eroding by 1 to fill any gaps, and finally manually editing the edges to exclude voxels in the ventricles and outside the brain. This resulted in a generous gray matter mask to restrict further analyses, which is also included in the online supplement. Finally, CBF maps were spatially smoothed using a 4 mm full-width half-maximum gaussian kernel.

2.7 | Whole brain voxel-wise group analyses

Using a general linear model (GLM), we conducted voxel-wise multiple linear regression across gray matter for the independent variables of infant age at scan, infant sex, Negative Affect Reactivity, and Positive Affect Recovery during the SFP-R, and each factor

extracted from the temperament EFA. Resulting statistical maps for each independent variable were then clustered and regional CBF values from each infant were extracted. Clusters were considered significant at FWE corrected $p < .05$, voxel-wise $p < .001$. We used AFNI's 3dFWHMx and 3dClustSim to estimate spatial autocorrelation function (ACF) parameters for the CBF data and an appropriate cluster size to minimize the false-positive rate (Cox, Chen, Glen, Reynolds, & Taylor, 2017). This method was developed specifically to minimize false-positives in clustering based on recent work demonstrating that BOLD fMRI noise does not fit a Gaussian distribution (Eklund, Nichols, & Knutsson, 2016). These ACF parameters were used to generate 10,000 Monte Carlo simulations in order to produce an estimate of cluster size that is conservative, minimizing the false-positive rate. The simulations returned a conservative cluster size of 98.6 voxels for a cluster-wise threshold of $p < .05$ and voxel-wise threshold of $p < .001$. However, due to the small size of infant brains, the unclear comparability of BOLD and ASL signal noise, and the exploratory nature of this analysis, clusters meeting an exploratory minimum threshold of 25 voxels were also reported.

3 | RESULTS

3.1 | Temperamental affect analysis

There was a significant difference in temperamental falling reactivity between infants who did and who did not produce usable CBF data such that infants who were included in the MRI analysis had higher falling reactivity scores ($p = .038$). Distributions of scores for the IBQ-R-SF subscales are presented in Appendix V (Figure A4).

The parallel analysis scree plot (Appendix V, Figure A5) indicated that a two-factor model best fit the sample data. The two-factor EFA, however, was a poor fit to the data. Because the original IBQ-R analysis found a three-factor model to best fit the data, we also tested a three-factor model, which proved to be both a better fit to the data and more interpretable than the two-factor model. The three-factor EFA model had a TLI of 0.86, SRMSR of 0.07 and RMSEA of 0.08 (95% confidence interval = [0.04, 0.1]) indicating a reasonable to excellent fit to the data. We present the factor loadings in Figure 1. The first factor (eigenvalue = 2.43, 17% proportional variance explained) had high positive loadings (greater than 0.5) of Distress to Limitations and Sadness and negative loading of Falling Reactivity. Given that this factor captured an inverse relation between negative affectivity and affect regulation, it was labeled Negative Affect. The second factor (eigenvalue = 1.29, 9% proportional variance explained) had a positive loading greater than 0.5 for Soothability alone. The third factor (eigenvalue = 2.20, 16% proportional variance explained) had high positive loadings for Smiling and Laughter, High Intensity Pleasure, and Vocal Reactivity, largely replicating the Surgency factor found by Gartstein and Rothbart (2003). For comparative purposes, a confirmatory factor analysis is included in (Appendix VI and visualized in Figure A8).

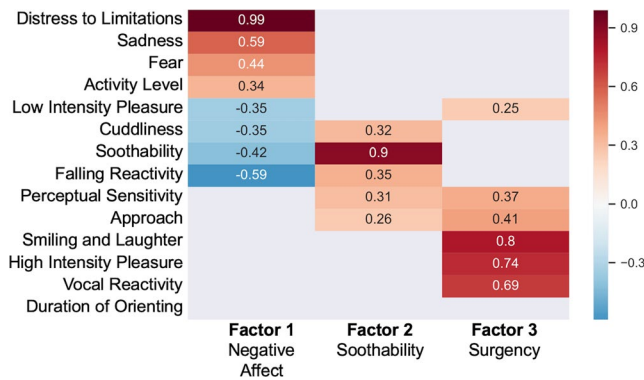


FIGURE 1 Factor structure for the Infant Behavior Questionnaire-Revised Short Form (IBQ-R-SF) derived from an exploratory three-factor analysis. Low loadings between -0.25 and 0.25 are omitted for clarity. Based on guidelines provided in de Winter, Dodou, and Wieringa (2009), this analysis is well-powered to detect loadings that are approximately 0.5 or higher

3.2 | Infant affect during the repeated Still-Face Paradigm

Replicating previous research, infants exhibited the “still-face” effect (i.e., increases in negative affect during still-face episodes and recovery of positive affect in reunion episodes) (Mesman et al., 2009) (Appendix V, Figure A6). Mean scores for Negative Affect Reactivity and Positive Affect Recovery during the SFP-R are presented in Table 1. There was no difference between infants who did and did not produce usable CBF data on either of these measures ($ps > 0.05$). The distributions for these two measures are presented in Appendix V (Figure A4).

Spearman's correlation tables for all five predictors in the general linear model ($N = 38$) as well as correlations for the 93 infants who completed the SFP-R are included in Table 2.

TABLE 2 Spearman correlations among the predictor variables included in the neuroimaging analysis ($N = 38$) and among all infants with both IBQ-R-SF and SFP-R data ($N = 93$)

	Positive recovery	Negative affect	Soothability	Surgency	Age
$N = 38$					
Negative reactivity	0.18	0.15	-0.08	0.35^{\dagger}	0.05
Positive recovery		-0.25	0.01	0.04	-0.18
Negative affect			-0.08	0.06	0.11
Soothability				-0.15	0.02
Surgency					0.44^*
$N = 93$					
Negative reactivity	-0.07	0.04	-0.11	0.01	0.00
Positive recovery		-0.17	-0.06	0.13	0.11
Negative affect			-0.02	-0.02	-0.03
Soothability				0.02	0.01
Surgency					0.18

Abbreviations: IBQ-R-SF, Infant Behavior Questionnaire-Revised Short Form; SFP-R, Still-Face Paradigm.

$^{\dagger}p < .05$,

$^*p < .01$.

3.3 | Whole brain voxel-wise group analyses

3.3.1 | Associations of infant age with rCBF

After accounting for the other predictors in the model, infant age at scan was positively associated with almost every voxel in the analysis brain mask (peak $t(37) = 36.04$, $p < .001$). Re-analyzing the CBF data with only age and sex in the model yielded virtually identical results, with a higher statistical peak of $t(37) = 50.36$ for the age term in the model. To gain a better understanding of the nature of this relation, the age term t -statistic map from the age and sex only model was further thresholded at the 95th percentile ($t(37) = 37.2$) in order to isolate regions with the strongest linear relation with age. Clusters that survived this threshold are listed in Table 3. Both the original results and the thresholded analysis are projected onto cortical surface renderings in Figure 2. Twenty-nine cluster peaks were identified spanning primary and secondary sensory regions, including the cuneus, somatosensory, parietal, premotor, and supplementary motor cortices, as well as limbic subcortical and cortical regions including the orbitofrontal cortex (OFC) and hippocampus, and integrative regions such as the temporoparietal junction and cerebellum.

3.3.2 | Associations of infant affect and temperamental emotionality with rCBF

The full list of clusters associated with each affect measure, statistically controlling for age at scan and infant sex, at both the exploratory and conservative cluster size thresholds are included in Table 4. Negative Affect Reactivity during the SFP-R was not associated with any rCBF clusters; however, Positive Affect Recovery

Region	Peak t-statistic	Extent voxels	Coordinates			CBF Mean \pm SD ml 100 g ⁻¹ min ⁻¹
			X	Y	Z	
Bilateral cuneus	50.63	1,236	64	41	50	118.8 \pm 8.5
Right inferior temporal gyrus	50.02	191	86	47	37	111.0 \pm 7.4
Right inferior parietal lobule	49.38	520	84	39	54	116.4 \pm 5.7
Right cerebellum	47.23	171	78	40	31	102.5 \pm 8.2
Left superior/middle temporal gyrus	46.85	1,284	41	65	40	115.5 \pm 6.8
Left precuneus	45.65	84	57	37	62	111.6 \pm 7.8
Right inferior frontal gyrus	45.00	451	80	77	44	118.2 \pm 8.6
Left dorsal cingulate cortex	44.65	141	62	53	63	115.7 \pm 9.4
Left medial prefrontal cortex	43.56	115	63	85	47	130.8 \pm 11.6
Left lateral occipital cortex	42.59	120	45	40	46	118.5 \pm 7.4
Right middle temporal gyrus	42.23	95	86	67	40	117.6 \pm 8.0
Right inferior frontal gyrus	41.03	37	82	83	49	102.4 \pm 8.0
Right lateral occipital cortex	40.83	49	82	35	42	109.6 \pm 7.5
Right inferior parietal lobule	40.60	54	87	53	58	116.1 \pm 7.9
Left fusiform gyrus	40.02	75	50	47	36	114.0 \pm 9.8
Right temporoparietal junction	39.64	37	84	53	50	117.0 \pm 7.7
Right inferior frontal gyrus	38.94	39	83	61	53	123.4 \pm 8.1

Note: These clusters were generated by thresholding the statistical map for the age term at the 95th percentile before clustering (voxel-wise $t(37) > 37.2$, cluster-wise $p < .05$). Only cluster larger than 25 voxels are included in the table.

Abbreviation: CBF, cerebral blood flow.

was positively associated with widespread rCBF. Regions that met or exceeded the conservative cluster size (shown in Figure 3) included the left inferior frontal gyrus (IFG), right medial OFC, right medial dorsal cingulate, right IFG, bilateral precuneus, the left lingual gyrus, and the left inferior temporal gyrus, with the latter two clusters extending into the cerebellum. With respect to dimensions of temperamental affect, only Negative Affect and Surgency were associated with clusters that exceeded the conservative cluster size threshold. Temperamental Negative Affect

was positively associated with right medial OFC rCBF; Surgency was negatively associated with left posterior operculum and right intraparietal sulcus rCBF.

A follow-up voxel-wise analysis was conducted on residualized rCBF data to test the extent to which these findings were explained by global CBF (the overall CBF of each infant). Specifically, CBF was averaged across the voxels included in the gray matter mask for each infant and this mean CBF value was regressed from each voxel. The voxel-wise analysis procedure was repeated on these residualized data

Voxel-wise rCBF Increases with Infant Age

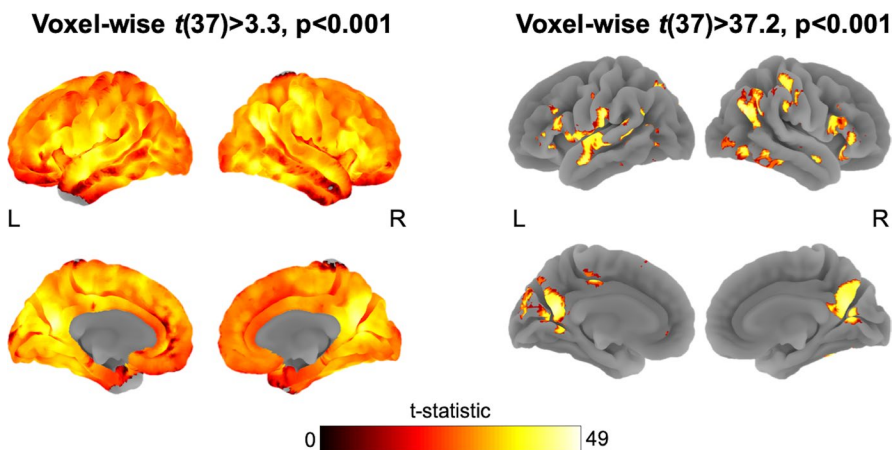


FIGURE 2 Almost every investigated voxel of gray matter cerebral blood flow (CBF) was positively associated with age after accounting for other predictors in the general linear model (GLM) (peak $t(37) = 41.2$, $p < .001$) and in a stand-alone re-analysis with only age and sex terms in the model (peak $t(37) = 50.4$, $p < .001$). 3a: The full statistical map thresholded at voxel-wise $p < .001$. 3b: the statistical map thresholded at the 95th percentile ($t(37) = 37.2$), highlighting cortical regions most significantly predicted by age at scan

TABLE 4 Cluster results from the group level general linear model, statistically controlling for age at scan and infant sex

Region	Peak t-statistic	Extent voxels	Coordinates			CBF Mean \pm SD ml 100 g ⁻¹ min ⁻¹
			X	Y	Z	
Positive Affect Recovery						
Left inferior frontal gyrus	6.69	134	38	67	57	94.97 \pm 8.10
Right inferior frontal gyrus	4.81	100	80	69	58	111.40 \pm 12.37
Right precuneus	4.70	77	72	48	68	101.42 \pm 12.81
Bilateral precuneus	4.37	102	64	40	58	120.93 \pm 9.61
Bilateral medial orbital frontal cortex	4.35	256	69	77	39	96.84 \pm 14.08
Left inferior frontal gyrus	4.29	158	44	69	50	115.70 \pm 10.15
Left lingual gyrus and cerebellum	4.26	228	62	48	40	103.35 \pm 10.72
Left inferior temporal gyrus	4.25	144	48	53	33	111.85 \pm 10.81
Left precentral gyrus	4.17	36	48	62	65	103.74 \pm 13.98
Right medial dorsal cingulate	4.13	260	71	59	62	108.67 \pm 10.88
Left mediodorsal thalamus	4.02	67	60	62	55	82.36 \pm 11.79
Right anterior insula	3.90	75	80	70	50	116.14 \pm 11.55
Left middle frontal gyrus	3.88	32	46	70	61	122.45 \pm 12.17
Right dorsal anterior cingulate	3.87	101	69	80	57	117.50 \pm 14.59
Right insula	3.78	27	82	64	50	117.01 \pm 10.81
Negative Affect Reactivity						
Left intraparietal sulcus	3.77	30	51	47	67	106.69 \pm 13.46
Temperamental Surgency						
Left posterior operculum	-4.86	199	49	52	57	86.99 \pm 13.86
Right intraparietal sulcus	-4.66	164	80	48	59	96.83 \pm 11.41
Temperamental Negative Affect						
Bilateral medial orbital frontal cortex	4.72	170	68	77	39	97.73 \pm 15.24
Temperamental Soothability						
Left inferior frontal gyrus	-3.99	42	45	81	44	87.93 \pm 12.44

Note: Significant clusters are voxel-wise $p < .001$, cluster FWE corrected $p < .05$. Clusters surviving the exploratory cluster size threshold of 25 are in plain text; clusters surviving the conservative 98.6-voxel threshold are in bold. Coordinates are given in the sample-specific template space, which is included in the online supplement.

Abbreviation: CBF, cerebral blood flow.

and the results are reported in Table 5. For context, the results of a general linear model testing the association among mean CBF and each variable included in the voxel-wise GLM is included in Appendix VII.

4 | DISCUSSION

The goal of this study was to identify the associations of age and affect with CBF in infants at a dynamic point in their brain development. The current findings increase our understanding of neural correlates of infant affect during the critical 5- to 8-months age range in infancy. We used multiple methods to measure infant affect reactivity and regulation, including both temperamental (i.e., global) and situational (i.e., in response to stress) affect reactivity

and regulation. Using a data-driven approach (factor analysis), we identified sample-specific dimensions of parent-reported infant temperamental emotionality. In addition, we objectively rated changes in infant affect during the SFP-R, a parent-child laboratory stressor. We then examined, for the first time, the associations of metrics of infant affect reactivity and regulation with infant rCBF, a measure of brain function that is not encumbered by the shifting relations among neuronal firing, oxygen consumption, and compensatory blood flow that adds non-uniform noise to the BOLD fMRI signal during infancy. Our findings suggest that greater rCBF is an indicator of greater tissue maturity and, further, that greater rCBF in several sensory, limbic, and prefrontal regions is associated greater Positive Affect Recovery following a stressor (main results and Appendix I). After correcting for global CBF, increased rCBF in

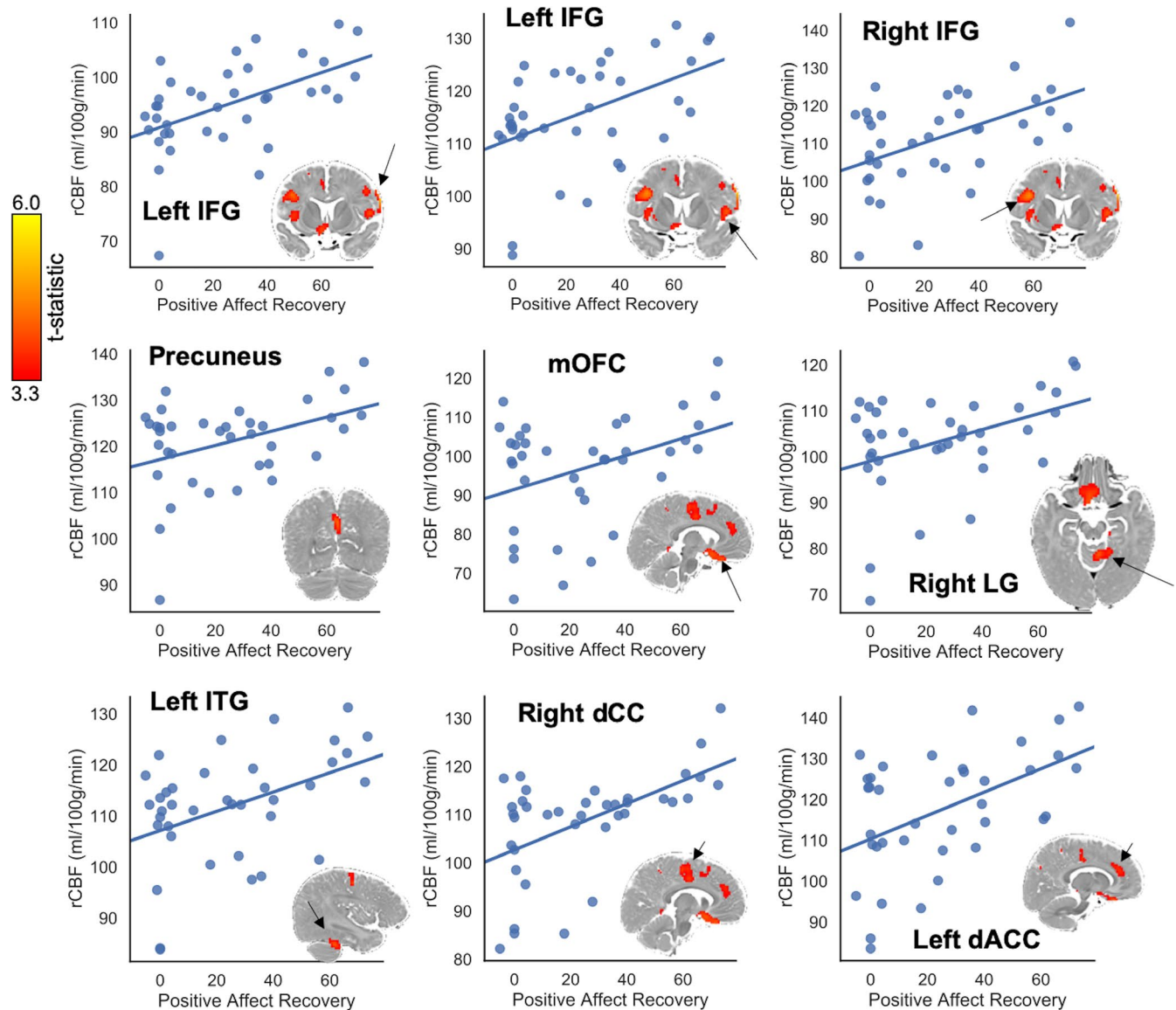


FIGURE 3 Cerebral blood flow (CBF) clusters associated with each affect measure that met the conservative 98.6 minimum cluster size. Clusters are FWE corrected $p < .05$, voxel-wise threshold $p < .001$. The scatterplot illustrates the positive linear association between the mean regional (rCBF) in these clusters and average increases in positive affect (Positive Affect Recovery) from the stressor to the reunion periods of the Still-Face Paradigm (SFP-R). The plotted cluster is indicated for each plot with a black arrow. dACC, dorsal anterior cingulate; dCC, medial dorsal cingulate; IFG, inferior frontal gyrus; ITG, inferior temporal gyrus; LG, lingual gyrus; mOFC, medial orbitofrontal cortex

nearly identical regions was associated with greater Temperamental Negative Affect. Together, these findings suggest an association between rCBF in affective regulatory regions (the orbitofrontal cortex and the inferior frontal gyrus) and specific infant experiences – expressing negative affect and experiencing affect regulation – that may indicate increased relative maturity of these brain regions as a result of having more of these experiences. Although we cannot draw causal conclusions from these data given the observational design of this study, these results provide important insight into which brain regions may underlie individual differences in affect reactivity and regulation in infants, complementing current models of affective development in infants and identifying targets for further study.

4.1 | Cerebral blood flow as a marker of tissue maturity in infancy

We identified a positive association between infant age (ranging from 5 to 8 months) and rCBF in almost every voxel we examined. This positive association between age and rCBF is consistent with previous research showing that capillary-level perfusion in the cortex increases across this age range (Harb et al., 2013; Kozberg & Hillman, 2016; Norman & O'kusky, 1986). Thus, our findings support the formulation that higher rCBF is an indicator of relatively more mature tissue. Indeed, we found that regions most strongly associated with age included the primary and secondary visual cortex, somatosensory cortex, parietal cortex, inferior frontal gyri, and the

TABLE 5 Results of the whole-brain voxel-wise analysis performed on the residuals (mean CBF regressed out)

Region	Peak t-statistic	Extent voxels	Coordinates		
			X	Y	Z
Negative Affect Reactivity					
Left inferior parietal lobule	5.29	99	48	50	65
Left inferior frontal gyrus	-4.66	60	37	65	55
Positive Affect Recovery					
Left cerebellum	4.14	27	61	49	40
Left temporal pole	-4.88	38	49	73	35
Temperamental Negative Affect					
Bilateral medial orbito-frontal cortex	4.99	188	68	77	39
Left lingual gyrus and cerebellum	4.34	54	59	49	42
Bilateral precuneus	4.00	63	64	49	62
Left precuneus	3.83	47	63	40	57
Left inferior frontal gyrus	-4.88	37	45	79	45
Left medial precentral gyrus	-4.29	25	60	55	69
Left occipital pole	-4.10	33	55	32	34
Temperamental Soothability					
Left precuneus/posterior cingulate	3.90	44	61	45	55
Temperamental Surgency					
Left cuneus	5.26	34	59	32	55
Right anterior operculum	4.36	86	78	80	48
Left posterior operculum	-5.53	182	48	51	57
Right intraparietal sulcus	-4.35	82	80	48	59

Note: As with the previously reported analysis, infant sex and age were included as covariates in the model. Consistent with Table 4, significant clusters are voxel-wise $p < .001$, cluster FWE corrected $p < .05$. Clusters surviving the exploratory cluster size threshold of 25 are in plain text; clusters surviving the conservative 98.6-voxel threshold are in bold. Coordinates are given in the sample-specific template space, which is included in the online supplement.

Abbreviation: CBF, cerebral blood flow.

superior temporal sulcus. These areas support skills that develop rapidly in infants, including visual (Kamitani & Tong, 2005), linguistic (Hickok & Poeppel, 2007), and self-regulatory (Fitzgerald et al., 2011; Quirk, Garcia, & González-Lima, 2006) processing.

4.2 | The orbitofrontal cortex and infant emotion

Both parent-assessed Temperamental Negative Affect and Positive Affect Recovery from a stressor predicted rCBF in large regions of the ventral medial OFC. The OFC was also a peak region most strongly

associated with infant age. The OFC is the limbic cortex of the PFC with direct innervation to and from the amygdala, insula, striatum, and visceral regions of the brainstem (Kalin, Shelton, & Davidson, 2007; Ongur & Price, 2000; Price, 2006). Data from lesion studies suggest that the OFC is an important mediator of anxious temperament and threat-response behavior in childhood and adolescence (Kalin et al., 2007). Furthermore, animal studies show that the OFC directly mediates amygdala response by adjusting emotional reactivity based on past learning (Pattwell et al., 2012; Quirk et al., 2006; Sotres-Bayon & Quirk, 2010). In humans, the OFC is among the first regions of the PFC to reach peak growth in early childhood (Shaw et al., 2008) and, therefore, may also be among the first prefrontal regions to develop in terms of both neurovasculature and neuronal-hemodynamic coupling. Indeed, some functional connectivity of the OFC with the amygdala is evident in children as young as 1 month of age, with dramatic refinement across the first year (Salzwedel et al., 2018) and increases in connectivity strength across childhood and adolescence (Gabard-Durnam et al., 2014; Jalbrzikowski et al., 2017). In contrast, other prefrontal regions such as the dorsolateral PFC do not appear to show stable functional connections until 1 year of age (Gao, Alcauter, Elton, et al., 2015; Gao, Alcauter, Smith, Gilmore, & Lin, 2015). Based on an understanding that greater CBF in the OFC in infancy may indicate greater tissue maturity and that the OFC is involved in emotion regulation, it is possible that infants who were rated as high in Temperamental Negative Affect and/or who were observed to recover well following a stressor are relatively more advanced in the development of limbic circuitry. In other words, the individual differences in rCBF of the OFC associated with infant affect may reflect individual differences in tissue maturity above and beyond those explained by chronological age.

4.3 | The inferior frontal gyrus in emotion regulation

Increased Positive Affect Recovery after the stressor was associated with increased rCBF in a large area of the IFG. There is evidence that the IFG plays two important roles in affect cognition: emotion identification and explicit emotion regulation. Lesion studies of the IFG suggest that the IFG is essential for participating in emotional empathy (Shamay-Tsoory, Aharon-Peretz, & Perry, 2009), specifically for processing prosody, the emotional component of speech (Frühholz & Grandjean, 2013; Rota, Handjaras, Sitaram, Birbaumer, & Dogil, 2011), and both identifying and creating emotional expressions (Hennenlotter et al., 2005). Furthermore, the IFG is consistently found to activate under directed emotion regulation conditions (Dörfel et al., 2014; Goldin, McRae, Ramel, & Gross, 2008; Grecucci, Giorgetta, Bonini, & Sanfey, 2013; Sarkheil, Klasen, Schneider, Goebel, & Mathiak, 2018) likely through connections to the insula and amygdala (Shiba et al., 2017). Like much of the PFC, the IFG has a protracted functional and structural development across childhood and adolescence (Ahmed, Bittencourt-Hewitt, & Sebastian, 2015; Camacho, Karim, & Perlman, 2019; Casey, Tottenham, Liston, & Durston, 2005; Shaw et al., 2008; Tsujimoto, 2008). Given that both

emotion identification and regulation dramatically improve between ages 3 and 10 months (Balaban, 1995; Caron et al., 1988; Feldman, Greenbaum, & Yirmiya, 1999; Kreutzer & Charlesworth, 1973), the observed positive association between Positive Affect Recovery and rCBF in the IFG may indicate relatively advanced local functional development of the IFG in infants who show greater recovery of positive affect following a stressor. Supporting this interpretation, we observed a strong positive association between age and IFG rCBF. This striking development is further supported by evidence from studies using resting state fMRI demonstrating that the frontoparietal functional network, which is thought to represent the communication of the prefrontal regulatory and the parietal integration regions, is still maturing at 1 year of age (Gao, Alcauter, Elton, et al., 2015; Gao, Lin, Grewen, & Gilmore, 2017). Further there is evidence implicating IFG function during social referencing in 15-month-old infants (Grossmann & Johnson, 2010). Increasing local blood flow is likely part of this important cognitive development.

4.4 | Emphasis on infant experience in the dyadic context

In this study, we found associations between CBF in regions associated with automatic regulation and parent-report and observational measures that index, in part, infant affect regulation (Positive Affect Recovery and Temperamental Negative Affect). Although these measures were largely unrelated to observed parenting behaviors in our sample (see Appendix III), they are contextualized in the infant-caregiver relationship through either caregiver perceptions (parent-reported temperament) or standardized parent-infant interaction (the Still-Face Procedure). Thus, our results may indicate that individual differences in affect expressed – and regulated – within the infant-caregiver context are linked to the relative functional maturity of self-regulatory and perceptual brain systems. The interpretation that our results reflect correlates of the infant's experience within the context of the dyad is consistent with what is known about the brain regions that were associated with Positive Affect Recovery and Temperamental Negative Affect. As we noted above, both the OFC and the IFG are implicated in affect regulation across social and non-social situations. In addition to these regions, rCBF in the lingual gyrus, a region of the primary visual cortex, was also associated with Positive Affect Recovery. The lingual gyrus forms a continuous structure with the parahippocampal gyrus, closely connecting it to the limbic system; there is evidence to suggest that this region is critical for both forming emotional memories and recognizing previously encountered emotional stimuli (Erk et al., 2003; Taylor et al., 1998). It is possible, therefore, that our findings reflect the neurobiological consequences of caregiver emotional responsiveness to infant negative affect; that is, children who express higher levels of negative affect observed by the parent may receive greater regulation from parents in response. In turn, children who express greater negative affect in their daily

lives may have more frequent opportunities to exercise these self-regulatory circuits, reinforcing existing connections and spurring further growth. Importantly, this model emphasizes the mutual contributions of the caregiving and the infant to affective neurodevelopment. Infants who do not respond to caregiver efforts are unlikely to benefit from them, and, therefore, would not demonstrate relative maturation of self-regulatory circuitry. Longitudinal studies – preferably research that also incorporates measures of dyadic interaction across a typical day – are needed to test this model more explicitly and systematically.

4.5 | Limitations and strengths

We should note four limitations of this study. First, in order to minimize total scan time for each infant, we captured only one snapshot of CBF. Therefore, we could not examine the temporal dynamics of regional CBF in this sample. Future studies should use ASL techniques that allow for a full timeseries to be collected and analyzed. Such data could inform our understanding of the network development across infancy found using BOLD fMRI. Second, this study was cross-sectional in design. Additional longitudinal research is necessary to draw strong conclusions about the temporal relation between brain development and emotional development in infancy. Third, while we believe we are justified in our formulation that increased rCBF is associated with cortical functional maturity, until such an association is empirically determined through longitudinal work this interpretation should be treated with caution. Furthermore, although it is likely that the association between rCBF during sleep and wake in 5- to 8-month-olds is generally comparable to the decreases in global CBF found in adults during sleep versus wakefulness (Hofle et al., 1997; Ktonas, Fagioli, & Salzarulo, 1995; Lenard, 1970; Madsen et al., 1991; Meyer, Ishikawa, Hata, & Karacan, 1987), equivalence between adults and infants in rCBF during sleep versus wake is only an assumption at this point. We could not compare infant rCBF during sleep versus wake in the current study given the challenges of scanning awake infants. Finally, as is the case with any neuroimaging analysis, there is a question of the specificity of our results. It is possible that the association between rCBF and infant affect is also related to other individual differences (e.g., in cognitive or motor development) that were not examined in this study. Despite these limitations, there are notable strengths of this study. For example, this is one of the first studies of infant CBF collected during natural sleep in healthy, at-term infants, and the first study to relate CBF to infant affect. Thus, this study adds to a small but growing body of literature indicating that CBF is a promising measure for elucidating normative early brain development (see Bouyssi-Kobar et al., 2018; Kim et al., 2018; Liu et al., 2019). We also used two common measures of infant affect, increasing the generalizability of our findings to studies of the neural correlates of infant affect. Importantly, we identified a three-factor structure of the IBQ-R in the current sample similar to the original

three-factor structure (Gartstein & Rothbart, 2003; Putnam et al., 2014) with a few key differences. Finally, we used cutting edge methods to quantify CBF in infants by creating a sample-specific analysis space and by quantifying T1 in a subset of the infant sample to use in kinetic modeling of rCBF. Mean whole brain rCBF for this sample is visualized in Appendix V (Figure A7).

5 | CONCLUSIONS

This is the first study to examine infant affect in relation to CBF during the critical 5- to 8-month period for emotional development, and represents an important step in understanding how early emotional experience shapes brain development. This study advances our understanding of affective neurodevelopment during a critical point in infant brain and emotional development. Specifically, existing BOLD fMRI work can now be interpreted with the added knowledge that it is likely that perfusion in the infant cortex increases across the 5- to 8-month age range in a non-uniform manner as we found here. Addressing gaps our knowledge related to the neural basis of infant emotion is critical given that maladaptive emotional tendencies in infancy can portend increased risk for the subsequent development of mood and disruptive disorders (Goldsmith & Alansky, 1987; Nigg, 2006; Rothbart & Ahadi, 1994; Winsper & Wolke, 2014; Zeanah, Boris, & Scheeringa, 1997). Future research focused on the early development of regions implicated in infant emotion in the current analysis, including the IFG and the OFC, could help to elucidate etiological processes in psychopathology and to identify targets for parent-child interventions.

ACKNOWLEDGEMENTS

This work was supported by the National Institutes of Health [R21 HD090493 to IHG, R21 MH111978 to IHG, and F32 MH107129], the National Science Foundation [Graduate Research Fellowships to MCC and LSK], and the Jacobs Foundation [Early Career Research Fellowship 2017-1261-05 to KLH]. The authors thank many families who donated their time to this project. We thank Hua Wu for her assistance and guidance with quantitative T1 imaging acquisition and analysis. We thank Monica Ellwood-Lowe, Sophie Schouboe, Vivian Vu, and Marissa Roth for their assistance with data collection.

CONFLICT OF INTEREST

The authors have no conflicts of interest to declare.

DATA AVAILABILITY STATEMENT

The data that support the findings of this study are available from the senior author Dr. Ian Gotlib (ian.gotlib@stanford.edu) upon reasonable request.

ORCID

M. Catalina Camacho  <https://orcid.org/0000-0003-0457-5410>

Lucinda M. Sisk  <https://orcid.org/0000-0003-4900-9770>

Kathryn L. Humphreys  <https://orcid.org/0000-0002-5715-6597>

REFERENCES

- Ahmed, S. P., Bittencourt-Hewitt, A., & Sebastian, C. L. (2015). Neurocognitive bases of emotion regulation development in adolescence. *Developmental Cognitive Neuroscience, 15*, 11–25. <https://doi.org/10.1016/j.dcn.2015.07.006>
- Alsop, D. C., Detre, J. A., Golay, X., Günther, M., Hendrikse, J., Hernandez-Garcia, L., ... Zaharchuk, G. (2015). Recommended implementation of arterial spin-labeled Perfusion MRI for clinical applications: A consensus of the ISMRM Perfusion Study group and the European consortium for ASL in dementia. *Magnetic Resonance in Medicine, 73*(1), 102–116. <https://doi.org/10.1002/mrm.25197>
- Andersson, J. L. R., Skare, S., & Ashburner, J. (2003). How to correct susceptibility distortions in spin-echo echo-planar images: Application to diffusion tensor imaging. *NeuroImage, 20*(2), 870–888. [https://doi.org/10.1016/S1053-8119\(03\)00336-7](https://doi.org/10.1016/S1053-8119(03)00336-7)
- Arichi, T., Fagiolo, G., Varela, M., Melendez-Calderon, A., Allievi, A., Merchant, N., ... Edwards, A. D. (2012). Development of BOLD signal hemodynamic responses in the human brain. *NeuroImage, 63*(2), 663–673. <https://doi.org/10.1016/j.neuroimage.2012.06.054>
- Arichi, T., Moraux, A., Melendez, A., Doria, V., Groppo, M., Merchant, N., ... Edwards, A. D. (2010). Somatosensory cortical activation identified by functional MRI in preterm and term infants. *NeuroImage, 49*(3), 2063–2071. <https://doi.org/10.1016/j.neuroimage.2009.10.038>
- Arthurs, O. J., & Boniface, S. (2002). How well do we understand the neural origins of the fMRI BOLD signal? *Trends in Neurosciences, 25*, 27–31. Retrieved from <http://tins.trends.com>
- Avants, B. B., Tustison, N. J., Song, G., Cook, P. A., Klein, A., & Gee, J. C. (2011). A reproducible evaluation of ANTs similarity metric performance in brain image registration. *NeuroImage, 54*(3), 2033–2044. <https://doi.org/10.1016/j.neuroimage.2010.09.025>
- Balaban, M. T. (1995). Affective influences on startle in five-month-old infants: Reactions to facial expressions of emotion. *Child Development, 66*(1), 28. <https://doi.org/10.2307/1131188>
- Barral, J. K., Gudmundson, E., Stikov, N., Etezadi-Amoli, M., Stoica, P., & Nishimura, D. G. (2010). A robust methodology for in vivo T1 mapping. *Magnetic Resonance in Medicine, 64*(4), 1057–1067. <https://doi.org/10.1002/mrm.22497>
- Belsky, J., Friedman, S. L., & Hsieh, K.-H. (2001). Testing a core emotion-regulation prediction: Does early attentional persistence moderate the effect of infant negative emotionality on later development? *Child Development, 72*(1), 123–133. <https://doi.org/10.1111/1467-8624.00269>
- Born, A. P., Miranda, M. J., Rostrup, E., Toft, P. B., Peitersen, B., Larsson, H. B. W., & Lou, H. C. (2000). Functional magnetic resonance imaging of the normal and abnormal visual system in early life. *Neuropediatrics, 31*(1), 24–32. <https://doi.org/10.1055/s-2000-15402>
- Bosquet Enlow, M., Carter, A., Hails, K., King, L., & Cabrera, I. (2014). Parent-child interaction rating scales – Infant adaptation manual.
- Bosquet Enlow, M., Kitts, R. L., Blood, E., Bizarro, A., Hofmeister, M., & Wright, R. J. (2012). Maternal posttraumatic stress symptoms and infant emotional reactivity and emotion regulation. *Infant Behavior and Development, 34*(4), 487–503. <https://doi.org/10.1016/j.infbeh.2011.07.007>
- Bosquet Enlow, M., White, M. T., Hails, K., Cabrera, I., & Wright, R. J. (2016). The Infant Behavior Questionnaire-revised: Factor structure in a culturally and sociodemographically diverse sample in the United States. *Infant Behavior & Development, 43*, 24–35. <https://doi.org/10.1016/j.infbeh.2016.04.001>
- Bouyssi-Kobar, M., Murnick, J., Brossard-Racine, M., Chang, T., Mahdi, E., Jacobs, M., & Limperopoulos, C. (2018). Altered cerebral perfusion in infants born preterm compared with infants born full term. *The Journal of Pediatrics, 193*, 54–61.e2. <https://doi.org/10.1016/j.jpeds.2017.09.083>
- Camacho, M. C., Karim, H. T., & Perlman, S. B. (2019). Neural architecture supporting active emotion processing in children: A multivariate



- approach. *NeuroImage*, 188, 171–180. <https://doi.org/10.1016/j.neuroimage.2018.12.013>
- Caron, A. J., Caron, R. F., & MacLean, D. J. (1988). Infant discrimination of naturalistic emotional expressions: The role of face and voice. *Child Development*, 59(3), 604. <https://doi.org/10.2307/1130560>
- Casey, B. J., Tottenham, N., Liston, C., & Durston, S. (2005). Imaging the developing brain: What have we learned about cognitive development? *Trends in Cognitive Sciences*, 9(3), 104–110. <https://doi.org/10.1016/j.tics.2005.01.011>
- Cox, R. W., Chen, G., Glen, D. R., Reynolds, R. C., & Taylor, P. A. (2017). fMRI clustering in AFNI: False-positive rates redux. *Brain Connectivity*, 7(3), 152–171. <https://doi.org/10.1089/brain.2016.0475>
- Crockenberg, S. C., Leerkes, E. M., & Barrig JO, P. S. (2008). Predicting aggressive behavior in the third year from infant reactivity and regulation as moderated by maternal behavior. *Development and Psychopathology*, 20(1), 37–54. <https://doi.org/10.1017/S0954579408000023>
- Dai, Y., Shi, F., Wang, L., Wu, G., & Shen, D. (2013). iBEAT: A toolbox for infant brain magnetic resonance image processing. *Neuroinformatics*, 11(2), 211–225. <https://doi.org/10.1007/s12021-012-9164-z>
- Damasio, A. R., Grabowski, T. J., Bechara, A., Damasio, H., Ponto, L. L. B., Parvizi, J., & Hichwa, R. D. (2000). Subcortical and cortical brain activity during the feeling of self-generated emotions. *Nature Neuroscience*, 3(10), 1049–1056. <https://doi.org/10.1038/79871>
- Datavyu Team. (2014). *Datavyu: A video coding tool*. New York, NY: New York University.
- Dean, D. C., O'Muirheartaigh, J., Dirks, H., Travers, B. G., Adluru, N., Alexander, A. L., & Deoni, S. C. L. (2016). Mapping an index of the myelin g-ratio in infants using magnetic resonance imaging. *NeuroImage*, 132, 225–237. <https://doi.org/10.1016/j.neuroimage.2016.02.040>
- Deen, B., Richardson, H., Dilks, D. D., Takahashi, A., Keil, B., Wald, L. L., ... Saxe, R. (2017). Organization of high-level visual cortex in human infants. *Nature Communications*, 8, 1–10. <https://doi.org/10.1038/ncomms13995>
- de Winter, J.C.F., Dodou, D., & Wieringa, P.A. (2009). Exploratory Factor Analysis With Small Sample Sizes. *Multivariate Behavioral Research*, 44(2), 147–181. <https://doi.org/10.1080/00273170902794206>
- Dörfel, D., Lamke, J.-P., Hummel, F., Wagner, U., Erk, S., & Walter, H. (2014). Common and differential neural networks of emotion regulation by detachment, reinterpretation, distraction, and expressive suppression: A comparative fMRI investigation. *NeuroImage*, 101, 298–309. <https://doi.org/10.1016/j.neuroimage.2014.06.051>
- Doria, V., Beckmann, C. F., Arichi, T., Merchant, N., Groppo, M., Turkheimer, F. E., ... Edwards, A. D. (2010). Emergence of resting state networks in the preterm human brain. *Proceedings of the National Academy of Sciences of the United States of America*, 107(46), 20015–20020. <https://doi.org/10.1073/pnas.1007921107>
- Eklund, A., Nichols, T. E., & Knutsson, H. (2016). Cluster failure: Why fMRI inferences for spatial extent have inflated false-positive rates. *Proceedings of the National Academy of Sciences of the United States of America*, 113(28), 7900–7905. <https://doi.org/10.1073/pnas.1602413113>
- Erk, S., Kiefer, M., Grothe, J., Wunderlich, A. P., Spitzer, M., & Walter, H. (2003). Emotional context modulates subsequent memory effect. *NeuroImage*, 18(2), 439–447. [https://doi.org/10.1016/S1053-8119\(02\)00015-0](https://doi.org/10.1016/S1053-8119(02)00015-0)
- Feldman, R., Greenbaum, C. W., & Yirmiya, N. (1999). Mother-infant affect synchrony as an antecedent of the emergence of self-control. *Developmental Psychology*, 35(1), 223–231. <https://doi.org/10.1037/0012-1649.35.1.223>
- Fernald, A. (1993). Approval and disapproval: Infant responsiveness to vocal affect in familiar and unfamiliar languages. *Child Development*, 64(3), 657–674. <https://doi.org/10.1111/j.1467-8624.1993.tb02934.x>
- Fitzgerald, D. A., Arnold, J. F., Becker, E. S., Speckens, A. E. M., Rinck, M., Rijpkema, M., ... Tendolcar, I. (2011). How mood challenges emotional memory formation: An fMRI investigation. *NeuroImage*, 56, 1783–1790. <https://doi.org/10.1016/j.neuroimage.2011.02.061>
- Fransson, P., Skiold, B., Horsch, S., Nordell, A., Blennow, M., Lagercrantz, H., & Aden, U. (2007). Resting-state networks in the infant brain. *Proceedings of the National Academy of Sciences of the United States of America*, 104(39), 15531–15536. <https://doi.org/10.1073/pnas.0704380104>
- Frühholz, S., & Grandjean, D. (2013). Processing of emotional vocalizations in bilateral inferior frontal cortex. *Neuroscience & Biobehavioral Reviews*, 37(10), 2847–2855. <https://doi.org/10.1016/j.neubiorev.2013.10.007>
- Gabard-Durnam, L. J., Flannery, J., Goff, B., Gee, D. G., Humphreys, K. L., Telzer, E., ... Tottenham, N. (2014). The development of human amygdala functional connectivity at rest from 4 to 23 years: A cross-sectional study. *NeuroImage*, 95, 193–207. <https://doi.org/10.1016/j.neuroimage.2014.03.038>
- Gao, W., Alcauter, S., Elton, A., Hernandez-Castillo, C. R., Smith, J. K., Ramirez, J., & Lin, W. (2015). Functional network development during the first year: Relative sequence and socioeconomic correlations. *Cerebral Cortex*, 25(9), 2919–2928. <https://doi.org/10.1093/cercor/bhu088>
- Gao, W., Alcauter, S., Smith, J. K., Gilmore, J. H., & Lin, W. (2015). Development of human brain cortical network architecture during infancy. *Brain Structure and Function*, 220(2), 1173–1186. <https://doi.org/10.1007/s00429-014-0710-3>
- Gao, W., Gilmore, J. H., Giovanello, K. S., Smith, J. K., Shen, D., Zhu, H., & Lin, W. (2011). Temporal and spatial evolution of brain network topology during the first two years of life. *PLoS ONE*, 6(9), e25278. <https://doi.org/10.1371/journal.pone.0025278>
- Gao, W., Lin, W., Grewen, K., & Gilmore, J. H. (2017). Functional connectivity of the infant human brain: Plastic and modifiable. *Neuroscientist*, 23(2), 169–184. <https://doi.org/10.1177/1073858416635986>
- Gartstein, M. A., & Rothbart, M. K. (2003). Studying infant temperament via the Revised Infant Behavior Questionnaire. *Infant Behavior and Development*, 26(1), 64–86. [https://doi.org/10.1016/S0163-6383\(02\)00169-8](https://doi.org/10.1016/S0163-6383(02)00169-8)
- Geng, X., Gouttard, S., Sharma, A., Gu, H., Styner, M., Lin, W., ... Gilmore, J. H. (2012). Quantitative tract-based white matter development from birth to age 2 years. *NeuroImage*, 61(3), 542–557. <https://doi.org/10.1016/j.neuroimage.2012.03.057>
- Goldin, P. R., McRae, K., Ramel, W., & Gross, J. J. (2008). The neural bases of emotion regulation: Reappraisal and suppression of negative emotion. *Biological Psychiatry*, 63(6), 577–586. <https://doi.org/10.1016/j.biopsych.2007.05.031>
- Goldsmith, H. H., & Alansky, J. A. (1987). Maternal and infant temperamental predictors of attachment: A meta-analytic review. *Journal of Consulting and Clinical Psychology*, 55(6), 805–816. <https://doi.org/10.1037/0022-006X.55.6.805>
- Gorgolewski, K., Burns, C. D., Madison, C., Clark, D., Halchenko, Y. O., Waskom, M. L., & Ghosh, S. S. (2011). Nipype: A flexible, lightweight and extensible neuroimaging data processing framework in python. *Frontiers in Neuroinformatics*, 5, 13. <https://doi.org/10.3389/fninf.2011.00013>
- Graham, A. M., Pfeifer, J. H., Fisher, P. A., Carpenter, S., & Fair, D. A. (2015). Early life stress is associated with default system integrity and emotionality during infancy. *Journal of Child Psychology and Psychiatry*, 56(11), 1212–1222. <https://doi.org/10.1111/jcpp.12409>
- Grecucci, A., Giorgetta, C., Bonini, N., & Sanfey, A. G. (2013). Reappraising social emotions: The role of inferior frontal gyrus, temporo-parietal junction and insula in interpersonal emotion regulation. *Frontiers in Human Neuroscience*, 7, 523. <https://doi.org/10.3389/fnhum.2013.00523>
- Grossmann, T., Missana, M., & Krol, K. M. (2018). The neurodevelopmental precursors of altruistic behavior in infancy. *PLoS Biology*, 16(9), e2005281. <https://doi.org/10.1371/journal.pbio.2005281>
- Grossmann, T., Striano, T., & Friederici, A. D. (2005). Infants' electric brain responses to emotional prosody. *NeuroReport*, 16(16), 1825–1828. <https://doi.org/10.1097/01.wnr.0000185964.34336.b1>
- Grossmann, T., & Johnson, M.H. (2010). Selective prefrontal cortex responses to joint attention in early infancy. *Biology Letters*, 6(4), 540–543. <https://doi.org/10.1098/rsbl.2009.1069>



- Haley, D. W., & Stansbury, K. (2003). Infant stress and parent responsiveness: Regulation of physiology and behavior during still-face and reunion. *Child Development, 74*(5), 1534–1546. <https://doi.org/10.1111/1467-8624.00621>
- Harb, R., Whiteus, C., Freitas, C., & Grutzendler, J. (2013). In vivo imaging of cerebral microvascular plasticity from birth to death. *Journal of Cerebral Blood Flow & Metabolism, 33*(1), 146–156. <https://doi.org/10.1038/jcbfm.2012.152>
- Hennenlotter, A., Schroeder, U., Erhard, P., Castrop, F., Haslinger, B., Stoecker, D., ... Ceballosbaumann, A. (2005). A common neural basis for receptive and expressive communication of pleasant facial affect. *NeuroImage, 26*(2), 581–591. <https://doi.org/10.1016/j.neuroimage.2005.01.057>
- Hickok, G., & Poeppel, D. (2007). The cortical organization of speech processing. *Nature Reviews Neuroscience, 8*(5), 393–402. <https://doi.org/10.1038/nrn2113>
- Hillman, E. M. C. (2014). Coupling mechanism and significance of the BOLD signal: A status report. *Annual Review of Neuroscience, 37*(1), 161–181. <https://doi.org/10.1146/annurev-neuro-071013-014111>
- Hofle, N., Paus, T., Reutens, D., Fiset, P., Gotman, J., Evans, A. C., & Jones, B. E. (1997). Regional cerebral blood flow changes as a function of delta and spindle activity during slow wave sleep in humans. *The Journal of Neuroscience, 17*(12), 4800–4808. <https://doi.org/10.1523/JNEUROSCI.17-12-04800.1997>
- Humphreys, K. L., King, L. S., Choi, P., & Gotlib, I. H. (2018). Maternal depressive symptoms, self-focus, and caregiving behavior. *Journal of Affective Disorders, 238*, 465–471. <https://doi.org/10.1016/j.jad.2018.05.072>
- Huttenlocher, P. R. (1990). Morphometric study of human cerebral cortex development. *Neuropsychologia, 28*(6), 517–527. [https://doi.org/10.1016/0028-3932\(90\)90031-I](https://doi.org/10.1016/0028-3932(90)90031-I)
- Huttenlocher, P. R., de Courten, C., Garey, L. J., & Van der Loos, H. (1982). Synaptogenesis in human visual cortex – Evidence for synapse elimination during normal development. *Neuroscience Letters, 33*(3), 247–252. [https://doi.org/10.1016/0304-3940\(82\)90379-2](https://doi.org/10.1016/0304-3940(82)90379-2)
- Issard, C., & Gervain, J. (2018). Variability of the hemodynamic response in infants: Influence of experimental design and stimulus complexity. *Developmental Cognitive Neuroscience, 33*, 182–193. <https://doi.org/10.1016/j.dcn.2018.01.009>
- Jalbrzikowski, M., Larsen, B., Hallquist, M. N., Foran, W., Calabro, F., & Luna, B. (2017). Development of white matter microstructure and intrinsic functional connectivity between the amygdala and ventromedial prefrontal cortex: Associations with anxiety and depression. *Biological Psychiatry, 82*, 511–521. <https://doi.org/10.1016/j.biopsych.2017.01.008>
- Kalin, N. H., Shelton, S. E., & Davidson, R. J. (2007). Role of the primate orbitofrontal cortex in mediating anxious temperament. *Biological Psychiatry, 62*(10), 1134–1139. <https://doi.org/10.1016/j.biopsych.2007.04.004>
- Kamitani, Y., & Tong, F. (2005). Decoding the visual and subjective contents of the human brain. *Nature Neuroscience, 8*(5), 679–685. <https://doi.org/10.1038/nn1444>
- Kim, H. G., Lee, J. H., Choi, J. W., Han, M., Gho, S.-M., & Moon, Y. (2018). Multidelay arterial spin-labeling MRI in neonates and infants: Cerebral perfusion changes during brain maturation. *American Journal of Neuroradiology, 39*(10), 1912–1918. <https://doi.org/10.3174/ajnr.A5774>
- King, L. S., Humphreys, K. L., & Gotlib, I. H. (2019). The neglect-enrichment continuum: Characterizing variation in early caregiving environments. *Developmental Review, 51*, 109–122. <https://doi.org/10.1016/j.dr.2019.01.001>
- Knickmeyer, R. C., Gouttard, S., Kang, C., Evans, D., Wilber, K., Smith, J. K., ... Gilmore, J. H. (2008). A structural MRI study of human brain development from birth to 2 years. *Journal of Neuroscience, 28*(47), 12176–12182. <https://doi.org/10.1523/JNEUROSCI.3479-08.2008>
- Kozberg, M., Chen, B. R., DeLeo, S. E., Bouchard, M. B., & Hillman, E. M. C. (2013). Resolving the transition from negative to positive blood oxygen level-dependent responses in the developing brain. *Proceedings of the National Academy of Sciences of the United States of America, 110*(11), 4380–4385. <https://doi.org/10.1073/pnas.1212785110>
- Kozberg, M., & Hillman, E. (2016). Neurovascular coupling and energy metabolism in the developing brain. In K. Masamoto, H. Hirase, & K. Yamada (Eds.), *New horizons in neurovascular coupling: A bridge between brain circulation and neural plasticity* (1st edn., pp. 213–242). Amsterdam, Netherlands: Elsevier B.V. <https://doi.org/10.1016/bs.pbr.2016.02.002>
- Kreutzer, M. A., & Charlesworth, W. R. (1973). Infants' reactions to different expressions of emotions. Retrieved from <https://files.eric.ed.gov/fulltext/ED078914.pdf>
- Ktonas, P. Y., Fagioli, I., & Salzarulo, P. (1995). Delta (0.5–1.5 Hz) and sigma (11.5–15.5 Hz) EEG power dynamics throughout quiet sleep in infants. *Electroencephalography and Clinical Neurophysiology, 95*(2), 90–96. [https://doi.org/10.1016/0013-4694\(95\)00051-Y](https://doi.org/10.1016/0013-4694(95)00051-Y)
- Lenard, H. (1970). The development of sleep spindles in the EEG during the first two years of life. *Neuropediatrics, 1*(03), 264–276. <https://doi.org/10.1055/s-0028-1091818>
- Li, G., Nie, J., Wang, L., Shi, F., Lin, W., Gilmore, J. H., & Shen, D. (2013). Mapping region-specific longitudinal cortical surface expansion from birth to 2 years of age. *Cerebral Cortex, 23*(11), 2724–2733. <https://doi.org/10.1093/cercor/bhs265>
- Lindquist, K. A., Wager, T. D., Kober, H., Bliss-Moreau, E., & Barrett, L. F. (2012). The brain basis of emotion: A meta-analytic review. *Behavioral and Brain Sciences, 35*(03), 121–143. <https://doi.org/10.1017/S0140525X11000446>
- Linke, A. C., Wild, C., Zubiaurre-Elorza, L., Herzmann, C., Duffy, H., Han, V. K., ... Cusack, R. (2018). Disruption to functional networks in neonates with perinatal brain injury predicts motor skills at 8 months. *NeuroImage: Clinical, 18*, 399–406. <https://doi.org/10.1016/j.nicl.2018.02.002>
- Liu, P., Qi, Y., Lin, Z., Guo, Q., Wang, X., & Lu, H. (2019). Assessment of cerebral blood flow in neonates and infants: A phase-contrast MRI study. *NeuroImage, 185*, 926–933. <https://doi.org/10.1016/j.neuroimage.2018.03.020>
- Logothetis, N. K., Pauls, J., Augath, M., Trinath, T., & Oeltermann, A. (2001). Neurophysiological investigation of the basis of the fMRI signal. *Nature, 412*(6843), 150–157. <https://doi.org/10.1038/35084005>
- Madsen, P. L., Holm, S., Vorstrup, S., Friberg, L., Lassen, N. A., & Wildschjødtt, G. (1991). Human regional cerebral blood flow during rapid-eye-movement sleep. *Journal of Cerebral Blood Flow & Metabolism, 11*(3), 502–507. <https://doi.org/10.1038/jcbfm.1991.94>
- Mangelsdorf, S. C., Shapiro, J. R., & Marzolf, D. (1995). Developmental and temperamental differences in emotion regulation in infancy. *Child Development, 66*(6), 1817–1828. <https://doi.org/10.1111/j.1467-8624.1995.tb00967.x>
- Meek, J. H., Firbank, M., Elwell, C. E., Atkinson, J., Braddick, O., & Wyatt, J. S. (1998). Regional hemodynamic responses to visual stimulation in awake infants. *Pediatric Research, 43*(6), 840–843. <https://doi.org/10.1203/00006450-199806000-00019>
- Mesman, J., van IJzendoorn, M. H., & Bakermans-Kranenburg, M. J. (2009). The many faces of the Still-Face Paradigm: A review and meta-analysis. *Developmental Review, 29*(2), 120–162. <https://doi.org/10.1016/j.dr.2009.02.001>
- Meyer, J. S., Ishikawa, Y., Hata, T., & Karacan, I. (1987). Cerebral blood flow in normal and abnormal sleep and dreaming. *Brain and Cognition, 6*(3), 266–294. [https://doi.org/10.1016/0278-2626\(87\)90127-8](https://doi.org/10.1016/0278-2626(87)90127-8)
- Miller, N. V., Degnan, K. A., Hane, A. A., Fox, N. A., & Chronis-Tuscano, A. (2018). Infant temperament reactivity and early maternal caregiving: Independent and interactive links to later childhood attention-deficit/hyperactivity disorder symptoms. *Journal of Child Psychology and Psychiatry, 60*(1), 43–53. <https://doi.org/10.1111/jcpp.12934>
- Minagawa-Kawai, Y., van der Lely, H., Ramus, F., Sato, Y., Mazuka, R., & Dupoux, E. (2011). Optical brain imaging reveals general auditory and language-specific processing in early infant development. *Cerebral Cortex, 21*, 254–261. <https://doi.org/10.1093/cercor/bhq082>
- Morales, S., Fu, X., & Pérez-Edgar, K. E. (2016). A developmental neuroscience perspective on affect-biased attention. *Developmental Cognitive Neuroscience, 21*, 26–41. <https://doi.org/10.1016/j.dcn.2016.08.001>

- Nakato, E., Otsuka, Y., Kanazawa, S., Yamaguchi, M. K., & Kakigi, R. (2011). Distinct differences in the pattern of hemodynamic response to happy and angry facial expressions in infants – A near-infrared spectroscopic study. *NeuroImage*, 54(2), 1600–1606. <https://doi.org/10.1016/j.neuroimage.2010.09.021>
- Nigg, J. T. (2006). Temperament and developmental psychopathology. *Journal of Child Psychology and Psychiatry*, 47(3–4), 395–422. <https://doi.org/10.1111/j.1469-7610.2006.01612.x>
- Norman, M. G., & O'kusky, J. R. (1986). The growth and development of microvasculature in human cerebral cortex. *Journal of Neuropathology and Experimental Neurology*, 45(3), 222. <https://doi.org/10.1097/00005072-198605000-00003>
- Ongur, D., & Price, J. L. (2000). The organization of networks within the orbital and medial prefrontal cortex of rats, monkeys and humans. *Cerebral Cortex*, 10(3), 206–219. <https://doi.org/10.1093/cercor/10.3.206>
- Pattwell, S. S., Duhoux, S., Hartley, C. A., Johnson, D. C., Jing, D., Elliott, M. D., ... Lee, F. S. (2012). Altered fear learning across development in both mouse and human. *Proceedings of the National Academy of Sciences of the United States of America*, 109(40), 16318–16323. <https://doi.org/10.1073/pnas.1206834109>
- Paus, T., Collins, D., Evans, A., Leonard, G., Pike, B., & Zijdenbos, A. (2001). Maturation of white matter in the human brain: A review of magnetic resonance studies. *Brain Research Bulletin*, 54(3), 255–266. [https://doi.org/10.1016/S0361-9230\(00\)00434-2](https://doi.org/10.1016/S0361-9230(00)00434-2)
- Pessoa, L. (2017). A network model of the emotional brain. *Trends in Cognitive Sciences*, 21(5), 357–371. <https://doi.org/10.1016/j.tics.2017.03.002>
- Posner, M. I., Rothbart, M. K., Sheese, B. E., & Voelker, P. (2014). Developing attention: Behavioral and brain mechanisms. *Advances in Neuroscience*, 2014, 1–9. <https://doi.org/10.1155/2014/405094>
- Price, J. L. (2006). Comparative aspects of amygdala connectivity. *Annals of the New York Academy of Sciences*, 985(1), 50–58. <https://doi.org/10.1111/j.1749-6632.2003.tb07070.x>
- Putnam, S. P., Helbig, A. L., Gartstein, M. A., Rothbart, M. K., & Leerkes, E. (2014). Development and assessment of short and very short forms of the Infant Behavior Questionnaire-revised. *Journal of Personality Assessment*, 96(4), 445–458. <https://doi.org/10.1080/00223891.2013.841171>
- Quirk, G. J., Garcia, R., & González-Lima, F. (2006). Prefrontal mechanisms in extinction of conditioned fear. *Biological Psychiatry*, 60(4), 337–343. <https://doi.org/10.1016/j.biopsych.2006.03.010>
- Revelle, W. (2018). *Psych: Procedures for psychological, psychometric, and personality research*. Evanston, IL: Northwestern University. Retrieved from <https://cran.r-project.org/package=psych>
- Rosseel, Y. (2012). lavaan: An R package for structural equation modeling. *Journal of Statistical Software*, 48(2), 1–36. Retrieved from <http://www.jstatsoft.org/v48/i02/>
- Rota, G., Handjaras, G., Sitaram, R., Birbaumer, N., & Dogil, G. (2011). Reorganization of functional and effective connectivity during real-time fMRI-BCI modulation of prosody processing. *Brain and Language*, 117(3), 123–132. <https://doi.org/10.1016/j.bandl.2010.07.008>
- Rothbart, M. K., & Ahadi, S. A. (1994). Temperament and the development of personality. *Journal of Abnormal Psychology*, 103(1), 55–66. <https://doi.org/10.1037/0021-843X.103.1.55>
- Rothbart, M. K., & Posner, M. I. (2015). Temperament, attention, and developmental psychopathology. In D. Cicchetti & D.J. Cohen (Eds.) *Developmental psychopathology* (pp. 465–501). Hoboken, NJ: John Wiley & Sons, Inc. <https://doi.org/10.1002/9780470939390.ch11>
- Rothbart, M. K., Sheese, B. E., Rueda, M. R., & Posner, M. I. (2011). Developing mechanisms of self-regulation in early life. *Emotion Review*, 3(2), 207–213. <https://doi.org/10.1177/1754073910387943>
- Ruscio, J., & Roche, B. (2012). Determining the number of factors to retain in an exploratory factor analysis using comparison data of known factorial structure. *Psychological Assessment*, 24(2), 282–292. <https://doi.org/10.1037/a0025697>
- Salzwedel, A. P., Stephens, R. L., Goldman, B. D., Lin, W., Gilmore, J. H., & Gao, W. (2018). Development of amygdala functional connectivity during infancy and its relationship with 4-year behavioral outcomes. *Biological Psychiatry: Cognitive Neuroscience and Neuroimaging*, 4(1), 62–71. <https://doi.org/10.1016/j.bpsc.2018.08.010>
- Sarkheil, P., Klasen, M., Schneider, F., Goebel, R., & Mathiak, K. (2018). Amygdala response and functional connectivity during cognitive emotion regulation of aversive image sequences. *European Archives of Psychiatry and Clinical Neuroscience*, 269(7), 803–811. <https://doi.org/10.1007/s00406-018-0920-4>
- Schreiber, J.B., Nora, A., Stage, F.K., Barlow, E.A., & King, J. (2006). Reporting Structural Equation Modeling and Confirmatory Factor Analysis Results: A Review. *The Journal of Educational Research*, 99(6), 323–338. <https://doi.org/10.3200/JOER.99.6.323-338>
- Sengupta, P. (2013). The Laboratory Rat: Relating its age with human's. *International Journal of Preventive Medicine*, 4(6), 624–630.
- Shamay-Tsoory, S. G., Aharon-Peretz, J., & Perry, D. (2009). Two systems for empathy: A double dissociation between emotional and cognitive empathy in inferior frontal gyrus versus ventromedial prefrontal lesions. *Brain*, 132(3), 617–627. <https://doi.org/10.1093/brain/awn279>
- Shaw, P., Kabani, N. J., Lerch, J. P., Eckstrand, K., Lenroot, R., Gogtay, N., ... Wise, S. P. (2008). Neurodevelopmental trajectories of the human cerebral cortex. *Journal of Neuroscience*, 28(14), 3586–3594. <https://doi.org/10.1523/JNEUROSCI.5309-07.2008>
- Shiba, Y., Oikonomidis, L., Sawiak, S., Fryer, T. D., Hong, Y. T., Cockcroft, G., ... Roberts, A. C. (2017). Converging prefronto-insula-amygdala pathways in negative emotion regulation in Marmoset Monkeys. *Biological Psychiatry*, 82(12), 895–903. <https://doi.org/10.1016/j.biopsych.2017.06.016>
- Shiner, R. L., Buss, K. A., McClowry, S. G., Putnam, S. P., Saudino, K. J., & Zentner, M. (2012). What is temperament now? Assessing progress in temperament research on the twenty-fifth anniversary of Goldsmith et al. *Child Development Perspectives*, 6(4), 436–444. <https://doi.org/10.1111/j.1750-8606.2012.00254.x>
- Sosinsky, L. S., Marakovitz, S., & Carter, A. S. (2004). Parent-Child Interaction Rating Scales (PCIRS). Unpublished Manual. University of Massachusetts Boston. JOUR.
- Sotres-Bayon, F., & Quirk, G. J. (2010). Prefrontal control of fear: More than just extinction. *Current Opinion in Neurobiology*, 20(2), 231–235. <https://doi.org/10.1016/j.conb.2010.02.005>
- Striano, T., Kopp, F., Grossmann, T., & Reid, V. M. (2006). Eye contact influences neural processing of emotional expressions in 4-month-old infants. *Social Cognitive and Affective Neuroscience*, 1(2), 87–94. <https://doi.org/10.1093/scan/nsl008>
- Taylor, S. F., Liberzon, I., Fig, L. M., Decker, L. R., Minoshima, S., & Koeppe, R. A. (1998). The effect of emotional content on visual recognition memory: A PET activation study. *NeuroImage*, 8(2), 188–197. <https://doi.org/10.1006/nimg.1998.0356>
- Thomas, J. C., Letourneau, N., Campbell, T. S., Tomfohr-Madsen, L., & Giesbrecht, G. F. (2017). Developmental origins of infant emotion regulation: Mediation by temperamental negativity and moderation by maternal sensitivity. *Developmental Psychology*, 53(4), 611–628. <https://doi.org/10.1037/dev0000279>
- Tronick, E., Als, H., Adamson, L., Wise, S., & Brazelton, T. B. (1978). The infant's response to entrapment between contradictory messages in face-to-face interaction. *Journal of the American Academy of Child Psychiatry*, 17(1), 1–13. [https://doi.org/10.1016/S0002-7138\(09\)62273-1](https://doi.org/10.1016/S0002-7138(09)62273-1)
- Tsujimoto, S. (2008). The prefrontal cortex: Functional neural development during early childhood. *Neuroscientist*, 14(4), 345–358. <https://doi.org/10.1177/1073858408316002>
- Wang, L., Gao, Y., Shi, F., Li, G., Gilmore, J. H., Lin, W., & Shen, D. (2015). LINKS: Learning-based multi-source IntegratiON framework for Segmentation of infant brain images. *NeuroImage*, 108, 160–172. <https://doi.org/10.1016/j.neuroimage.2014.12.042>
- Wen, X., Zhang, H., Li, G., Liu, M., Yin, W., Lin, W., ... Shen, D. (2019). First-year development of modules and hubs in infant brain functional

- networks. *NeuroImage*, 185, 222–235. <https://doi.org/10.1016/j.neuroimage.2018.10.019>
- Winsper, C., & Wolke, D. (2014). Infant and toddler crying, sleeping and feeding problems and trajectories of dysregulated behavior across childhood. *Journal of Abnormal Child Psychology*, 42(5), 831–843. <https://doi.org/10.1007/s10802-013-9813-1>
- Worobey, J., & Blajda, V. M. (1989). Temperament ratings at 2 weeks, 2 months, and 1 year: Differential stability of activity and emotionality. *Developmental Psychology*, 25, 257–263. <https://doi.org/10.1037/0012-1649.25.2.257>
- Wu, H., Dougherty, R. F., Kerr, A. B., Zhu, K., & Middione, M. J. (2015). Fast T1 mapping using slice-shuffled simultaneous multi-slice inversion recovery EPI. *International Society for Magnetic Resonance in Medicine*, 1057(2010), 0440. Retrieved from <http://cds.ismrm.org/protected/15MPresentations/abstracts/0440.pdf>

- Yamada, H., Sadato, N., Konishi, Y., Kimura, K., Tanaka, M., Yonekura, Y., & Ishii, Y. (1997). A rapid brain metabolic change in infants detected by fMRI. *NeuroReport*, 8(17), 3775–3778. <https://doi.org/10.1097/00001756-199712010-00024>
- Zeanah, C. H., Boris, N. W., & Scheeringa, M. S. (1997). Psychopathology in infancy. *Journal of Child Psychology and Psychiatry*, 38(1), 81–99. <https://doi.org/10.1111/j.1469-7610.1997.tb01506.x>

How to cite this article: Camacho MC, King LS, Ojha A, et al. Cerebral blood flow in 5- to 8-month-olds: Regional tissue maturity is associated with infant affect. *Dev Sci*. 2019;00:e12928. <https://doi.org/10.1111/desc.12928>

APPENDIX I

VOXEL-WISE rCBF ANALYSIS USING THE STANDARD IBQ-R-SF FACTORS

As we described in the main text, the original IBQ-R-SF factor analysis yielded three factors (referred to as the “original” factors): Surgency, Negative Affect, and Self-Regulation (Putnam et al., 2014). To examine associations between these original factors and rCBF in these infants, we estimated factor scores from a confirmatory factor analysis with the original factor loadings. We used factor scores to aid in comparability with the main text analysis. We then entered these factor scores (Surgency, Negative Affect, and

Self-Regulation) into a voxel-wise linear model as described in the Whole Brain Voxel-Wise Group Analyses section of the main text, with the situational affect measures (Positive Affect Recovery and Negative Affect Reactivity) as well as age and sex. Results are listed in Table A1 below.

The specific regions identified as associated with Positive Affect Recovery are the same; no clusters survived either clustering threshold for the other affect measures in the model. These results are nearly identical to the results in the main text and suggest that individual differences in orbitofrontal cortex and inferior frontal gyrus maturation are critical in understanding affective development in infants, and in particular, recovery of affect following a stressor.

TABLE A1 Whole brain results using the original IBQ-R-SF factors

Region	Peak	Extent	Coordinates			rCBF
	t-statistic	Voxels	X	Y	Z	Mean ± SD
Positive Affect Recovery						
Left inferior frontal gyrus	7.29	390	38	67	57	107.8 ± 8.6
Right precuneus/superior parietal lobule	5.42	276	72	48	68	101.7 ± 11.5
Bilateral orbitofrontal cortex	5.33	366	67	77	38	97.6 ± 13.3
Right inferior and middle frontal gyri	4.76	113	80	69	58	112.8 ± 12.1
Left precentral gyrus	4.70	31	51	56	73	95.0 ± 12.8
Left precentral gyrus	4.63	83	48	62	65	102.1 ± 13.3
Right dorsal cingulate	4.63	782	72	61	63	111.5 ± 11.1
Bilateral precuneus	4.59	134	64	40	57	120.6 ± 9.8
Left thalamus, hippocampus, lingual gyrus, and cerebellum	4.58	1,323	60	63	55	100.2 ± 9.7
Left cuneus	4.36	100	58	32	57	110.7 ± 10.8
Left middle frontal gyrus	4.22	33	53	66	67	100.4 ± 12
Left cuneus	4.10	43	62	29	48	100.8 ± 7.5
Right insula	4.07	228	82	64	50	114.0 ± 9.9
Left middle temporal gyrus	3.87	44	41	66	35	99.2 ± 13.6
Right cuneus	3.73	25	70	31	56	114.8 ± 10.7

Note: Consistent with the analyses in the main text, clusters surviving the a priori cluster size threshold of 25 are included in plain text while clusters that exceeded the conservative voxel threshold of 98.6 are in bold. Only clusters for Positive Affect Recovery survived either threshold

APPENDIX II

INFANT OBSERVED AFFECT RELIABILITY CODING

Ten videos were randomly selected to be coded by a second rater. We estimated reliability by calculating the ICC for ratings assessing affect, ranging from hard crying (1) to very positive (6). These ratings were on an ordinal scale and were those we used to quantify affective reactivity and recovery. We did not include ratings for mixed affect, unobservable segments, unclassifiable segments, or autonomic indicators when calculating reliability.

	2	3	4	5	6	7	8
1. Maternal Sensitivity	-0.87	0.40	0.14	-0.10	0.04	0.06	-0.23
2. Maternal Intrusiveness	1.00	-0.17	-0.13	0.11	-0.03	-0.03	0.19
3. Maternal Warmth		1.00	0.01	0.22	-0.09	-0.01	-0.03
4. Negative Affect Reactivity			1.00	-0.10	-0.07	-0.07	-0.04
5. Positive Affect Recovery				1.00	-0.06	-0.06	0.11
6. Temperamental Negative Affect					1.00	0.00	0.00
7. Temperamental Soothability						1.00	0.04
8. Temperamental Surgency							1.00

Note: Significant correlations ($p < .05$) are bolded.

APPENDIX III

ANALYSIS OF CAREGIVING BEHAVIOR

As part of the broader study, we observationally coded maternal caregiving behavior during the SFP-R. As we have described previously (Humphreys et al., 2018; King et al., 2019), videos of the SFP-R were time-locked and bookmarked in Datavyu (Datavyu Team, 2014). Using the infant adaptation of the Parent - Child Interaction Rating Scales (Bosquet Enlow, Carter, Hails, King, & Cabrera, 2014; Sosinsky, Marakovitz, & Carter, 2004; <https://osf.io/gwpcj/>), trained

TABLE A2 Pearson's bivariate correlations among maternal caregiving ratings and each measure of infant affect

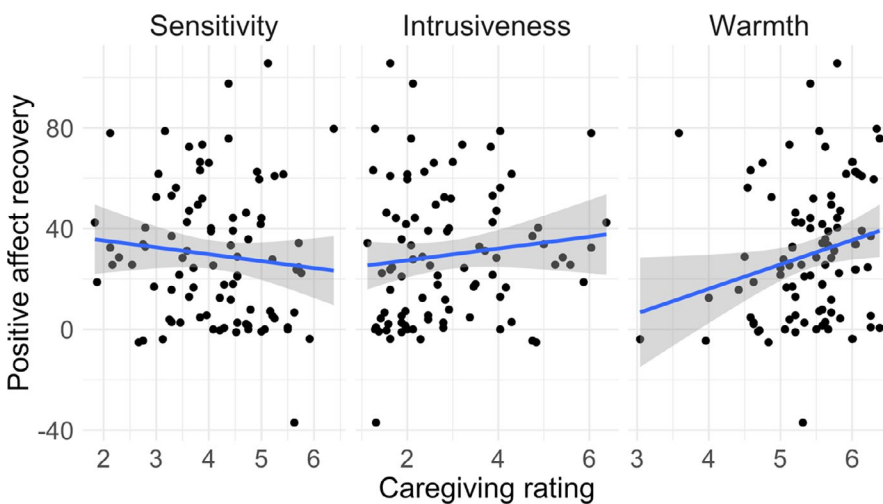


FIGURE A1 Associations between maternal caregiving ratings and Positive Affect Recovery

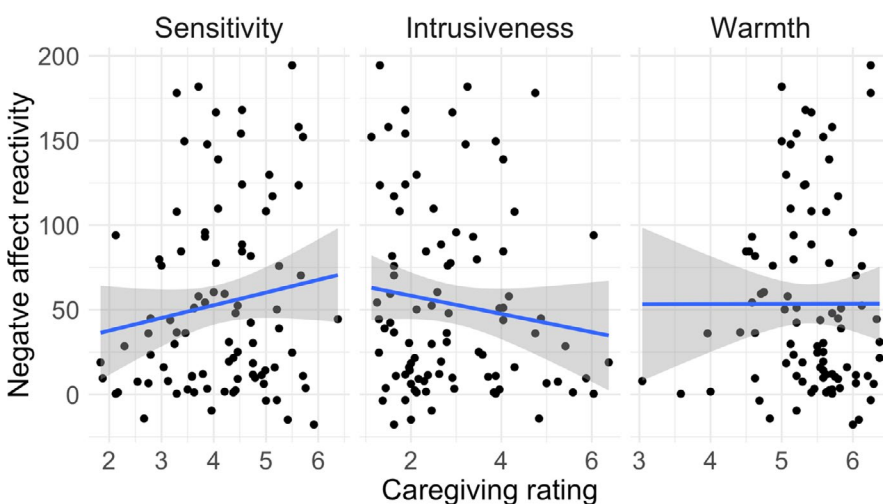


FIGURE A2 Associations between maternal caregiving ratings and Negative Affect Reactivity

TABLE A3 Demographic information for the subsample of infants included in the qT1 template creation

Demographic variable	Statistic
Infant age at scan, mean \pm SD weeks	6.76 \pm 0.68
Infant race, number (percent)	
White/Caucasian American	19 (65.5)
Asian American	6 (20.7)
Black/African American	3 (10.3)
Native Hawaiian/Pacific Islander	0 (0.0)
American Indian or Alaska Native	0 (0.0)
Other/biracial	1 (3.4)
Infant ethnicity, number (percent)	
Hispanic or Latinx	7 (24.1)
Not Hispanic or Latinx	21 (72.4)
Not provided	1 (3.4)
Annual household income, number (percent)	
Less than \$5,000	0 (0.0)
\$5,001–15,000	0 (0.0)
\$15,001–30,000	2 (6.9)
\$30,001–60,000	4 (13.8)
\$60,001–90,000	2 (6.9)
\$90,001–150,000	11 (37.9)
More than \$150,000	10 (34.5)
Decline to state	0 (0.0)
Infant sex, N male (percent)	17 (58.6)
Breastfed, number (percent)	
Yes	25 (86.2)
No	3 (10.3)
Not provided	1 (3.4)
Mother age, mean \pm SD years	32.96 \pm 4.92
Maternal race, number (percent)	
White/Caucasian American	18 (62.1)
Asian American	7 (24.1)
Black/African American	1 (3.4)
Native Hawaiian/Pacific Islander	0 (0.0)
American Indian or Alaska Native	0 (0.0)
Other/biracial	3 (10.3)
Maternal ethnicity, number (percent)	
Hispanic or Latinx	6 (20.7)
Not Hispanic or Latinx	23 (79.3)
Not provided	0 (0.0)
Maternal education, number (percent)	
Some high school	0 (0.0)
High school diploma/GED	0 (0.0)
Some college	0 (0.0)
Associate's degree	2 (6.9)
Trade/technical school	2 (6.9)
Bachelor's degree	11 (37.9)
Graduate degree	14 (48.3)

independent coders rated maternal sensitivity, intrusiveness, and positive regard (i.e., warmth) during each interval of the SFP-R, with possible scores ranging from 1 (not at all characteristic) to 7 (very characteristic), increasing in half-point increments (Humphreys et al., 2018). We computed the mean ratings of sensitivity, intrusiveness, and positive regard across all 30-s intervals in the two reunion episodes of the SFP-R. To ensure reliability, a subset of the SFP-R (16%) videos were selected to be rated by two coders. Reliability at the level of mean ratings was good (sensitivity ICC = 0.86; intrusiveness ICC = 0.87, warmth ICC = 0.84).

Using Pearson's bivariate correlations, we tested the association between each of the caregiving ratings and each of the infant affect measures (Negative Affect Reactivity, Positive Affect Recovery, Temperamental Surgency, Temperamental Negative Affect, Temperamental Soothability). We found no significant associations between sensitivity and intrusiveness and either Negative Affect Reactivity or Positive Affect Recovery (see Table A2 and Figures A1 and A2). Warmth was weakly positively associated with Positive Affect Recovery ($p = .034$) but was not associated with Negative Affect Reactivity. Temperamental Surgency was modestly associated with Sensitivity ($p = .026$).

APPENDIX IV

QUANTITATIVE T1 (qT1) TEMPLATE CREATION

Participants

The subset of infants included in the creation of the qT1 template were 29 5- to 8-month-olds. Their demographic information is presented below.

MR acquisition

Quantitative T1w images were collected using a simultaneous multi-slice IR-EPI with slice shuffling and a thin slice spiral spectral pulse (Wu, Dougherty, Kerr, Zhu, & Middione, 2015) with the following parameters (pe0): TR = 3.5 s, TE = 44 ms, matrix = 120 \times 120, resolution = 2 \times 2 mm², in-plane acceleration factor = 2, through-plane acceleration factor = 3, slice thickness = 2 mm, number of prescribed slices = 19, number of phases = 30. To correct for warping resulting from the quick acquisition, a shorter acquisition was collected in the opposite phase encoding direction (pe1), resulting in pair images with opposite distortions. Total acquisition time was 3 min, 50 s.

T1 quantification and template creation

T1 was quantified on a voxel-wise basis using a processing pipeline designed at the Center for Cognitive and Neurobiological Imaging at Stanford University for this specific acquisition, a multi-inversion-recovery (TI) EPI sequence (Wu et al., 2015). First, the pe1 volume and one volume from the pe0 acquisitions were used to estimate the susceptibility-induced off-resonance field (Andersson, Skare, & Ashburner, 2003) as implemented in FSL. This field was then applied to the full pe0 acquisition to effectively unwarped it. The resulting unwarped volume was then unshuffled and T1 was

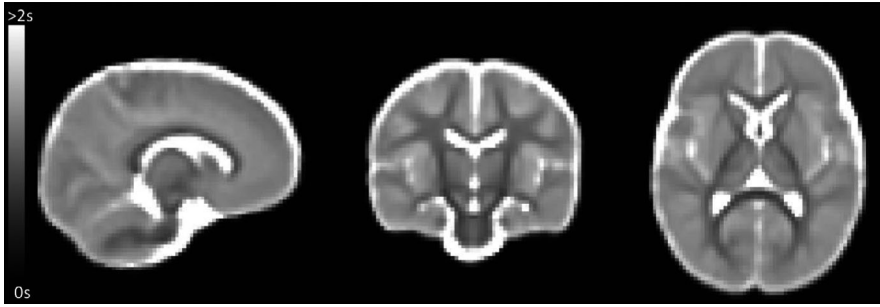


FIGURE A3 Average T1 created from a quantitative T1 sequence obtained from a subset of infants

quantified per previously published methods (Barral et al., 2010). All quantified participant volumes were visually inspected for motion artifacts before inclusion in the template creation procedure. Finally, all usable quantified T1 (qT1) images were used to make the sample-specific template using the ANTs multivariate template creation pipeline. This pipeline consists of iterative diffeomorphic registrations between each infant and eventual averaging to create

a sample-specific template (Avants et al., 2011). Images of the template are included below.

APPENDIX V

ADDITIONAL FIGURES

Scale/Score distributions

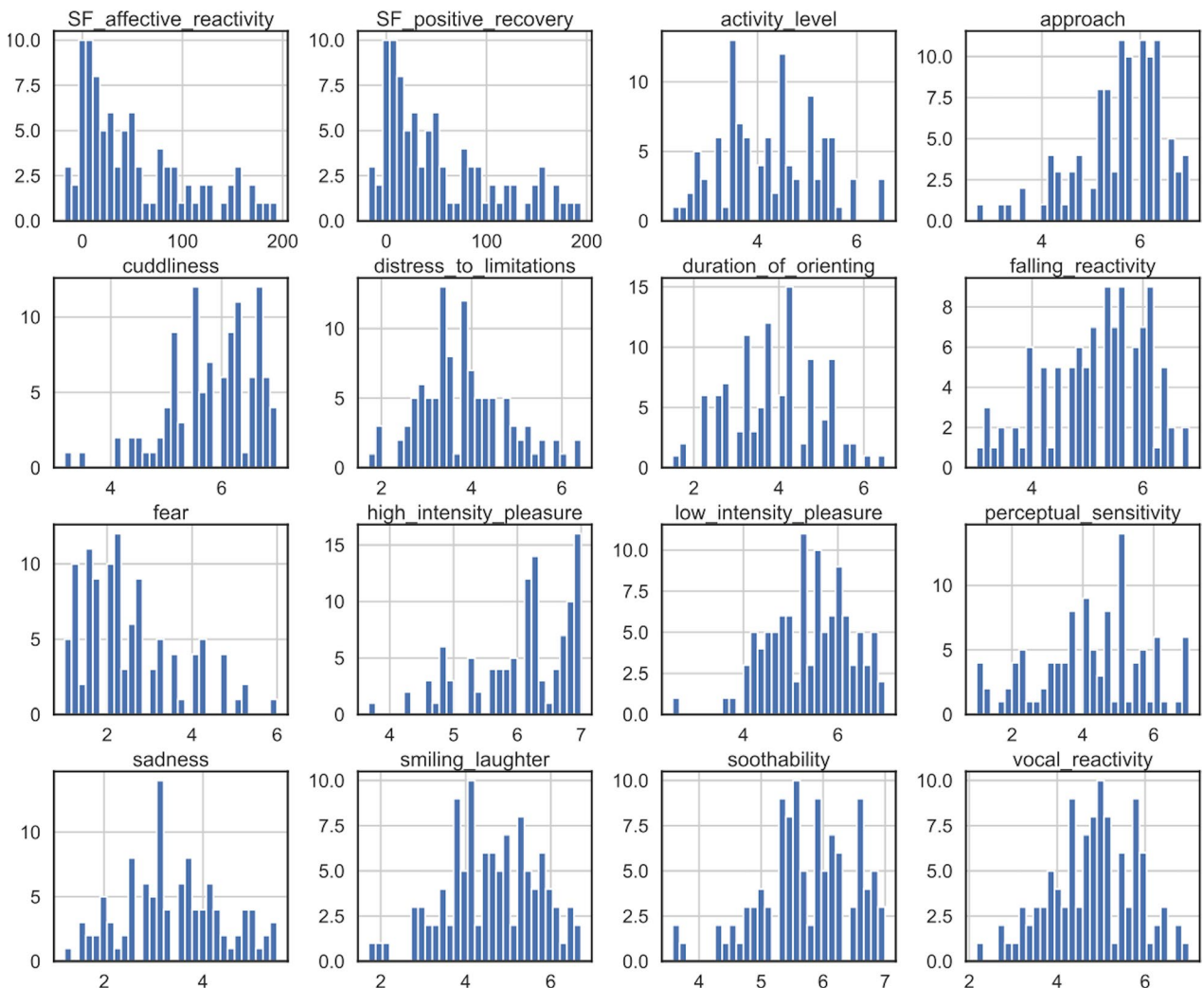
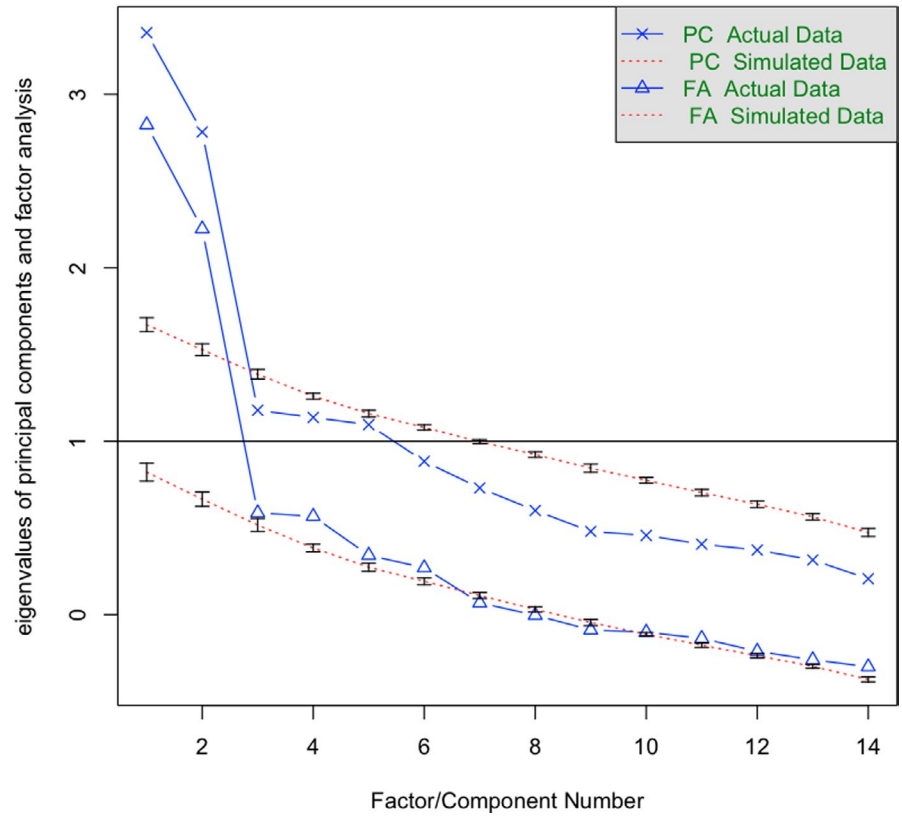


FIGURE A4 Histogram distributions for the affective codes from the Still-Face Paradigm (SF Negative Reactivity and SF Positive Recovery) and for each scale of the Infant Behavior Questionnaire-Revised, Short Form. Bin widths are plotted to fit 30 bins



FIGURE A5 Scree plots of actual and simulated factor analyses generated using the psych library in R. From this graphic, a 2-factor model was recommended for these data

Parallel Analysis Scree Plots



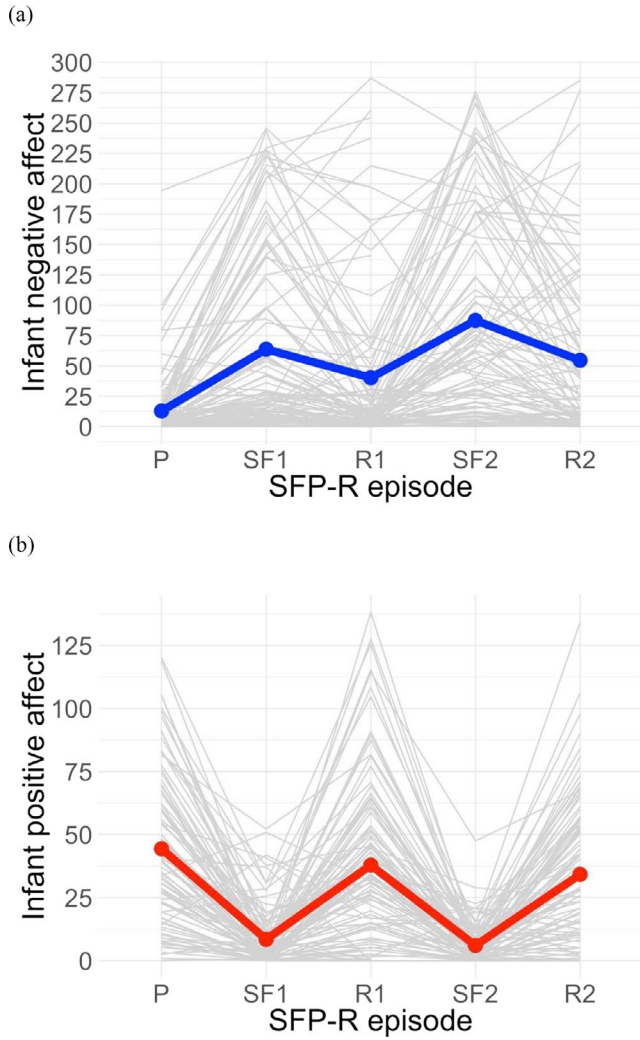
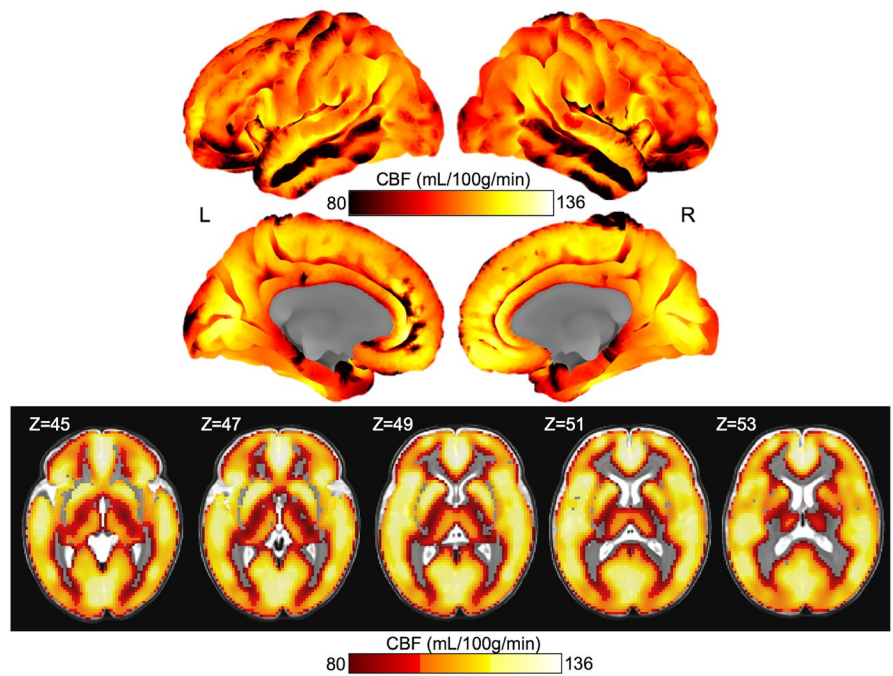


FIGURE A6 Infant positive and negative affect across the SFP-R in the full sample ($N = 93$). Notes: P = play, SF1 = first still-face, R1 = first reunion, SF2 = second still-face, R2 = second reunion. Replicating previous research, infants exhibited increased negative affect in still-face relative to non-still-face episodes and increased positive affect in reunion relative to still-face episodes

FIGURE A7 Whole brain rCBF projected onto the cortical surface and in slices. Cortical projections are colorbar centered at 80–136, thus regions that are black indicate an rCBF of 80 ml 100 g⁻¹ min⁻¹ or below. Slices of the insula and subcortical structures are included below the cortical surface projections with the Z-direction slice number indicated in the upper left corner of each image. The slice images are thresholded at 80 ml 100 g⁻¹ min⁻¹ for ease of reading, thus clear voxels on the overlay indicate either signal below 80 ml 100 g⁻¹ min⁻¹ or excluded voxels (such as in the case of white matter)



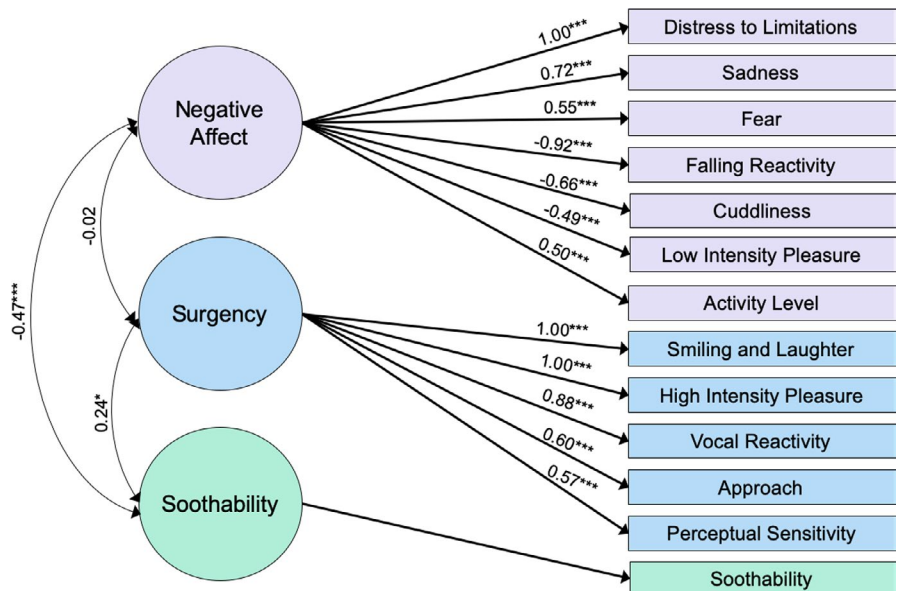
APPENDIX VI

CONFIRMATORY FACTOR ANALYSIS

Loadings from the 3-factor EFA with an absolute value greater than or equal to 0.3 were included in a confirmatory factor analyses (CFA)

to determine final model fit using the lavaan library (Rosseel, 2012) resulting in Duration of Orienting being removed from the model. The final 3-factor CFA results are depicted in below. The CFA model fit was a more modest fit than the EFA (TLI = 0.72, SRMSR = 0.10, RMSEA [90% CI] = 0.11 [0.09, 0.14]). All scales covaried significantly with their designated factors (*ps* < 0.001). Further, surgency and soothability positively covaried (standardized loading = 0.24, *p* < .01)

FIGURE A8 Final CFA for the 3-factor model. Standardized loading values are shown. Duration of Orienting was excluded from this model for not meeting the 0.3 threshold in the EFA. †*p* < .05; **p* < .01; ***p* < .005; ****p* < .001



and negative affect and soothability negatively covaried (standardized loading = -0.47 , $p < .001$).

APPENDIX VII

FOLLOW UP EXAMINATION OF GLOBAL CBF AND AFFECT MEASURES

Voxels within the generous gray matter mask were averaged for each individual infant. These mean CBF values were then entered as

the Y variable in a general linear model with the formula: $CBF \sim \text{age} + \text{sex} + \text{Positive Affect Recovery} + \text{Negative Affect Reactivity} + \text{Surgency} + \text{Negative Affect} + \text{Soothability}$. The Positive Affect Recovery term was weakly positively associated with mean CBF ($p = .048$) when all other terms were held constant. It is important to note that the mean CBF values include regions with only modest signal in its calculation that did not appear in the voxel-wise analysis.